



8-Benzylaminoxanthine scaffold variations for selective ligands acting on adenosine A_{2A} receptors. Design, synthesis and biological evaluation

Michał Załuski^a, Jakub Schabikowski^a, Piotr Jaśko^b, Adrian Bryła^b, Agnieszka Olejarz-Maciej^a, Maria Kaleta^a, Monika Głuch-Lutwin^c, Andreas Brockmann^d, Sonja Hinz^d, Małgorzata Zygmunt^b, Kamil Kuder^a, Gniewomir Latacz^a, Christin Vielmuth^d, Christa E. Müller^d, Katarzyna Kieć-Kononowicz^{a,*}

^a Department of Technology and Biotechnology of Drugs, Faculty of Pharmacy, Jagiellonian University Medical College, Medyczna 9, 30688 Kraków, Poland

^b Department of Pharmacodynamics, Faculty of Pharmacy, Jagiellonian University Medical College, Medyczna 9, 30688 Kraków, Poland

^c Department of Pharmacobiology, Faculty of Pharmacy, Jagiellonian University Medical College, Medyczna 9, 30688 Kraków, Poland

^d PharmaCenter Bonn, Pharmaceutical Institute, Pharmaceutical & Medicinal Chemistry, University of Bonn, An der Immenburg 4, 53121 Bonn, Germany

ARTICLE INFO

Keywords:

Adenosine A_{2A} receptors
Anti-inflammatory activity
Metabolic stability
Molecular docking
Monoamine oxidase
Phosphodiesterase
Xanthine derivatives

ABSTRACT

A library of 34 novel compounds based on a xanthine scaffold was explored in biological studies for interaction with adenosine receptors (ARs). Structural modifications of the xanthine core were introduced in the 8-position (benzylamino and benzyloxy substitution) as well as at N1, N3, and N7 (small alkyl residues), thereby improving affinity and selectivity for the A_{2A} AR. The compounds were characterized by radioligand binding assays, and our study resulted in the development of the potent A_{2A} AR ligands including 8-((6-chloro-2-fluoro-3-methoxybenzyl)amino)-1-ethyl-3,7-dimethyl-3,7-dihydro-1H-purine-2,6-dione (**12d**; K_i human A_{2A}AR: 68.5 nM) and 8-((2-chlorobenzyl)amino)-1-ethyl-3,7-dimethyl-3,7-dihydro-1H-purine-2,6-dione (**12h**; K_i human A_{2A}AR: 71.1 nM). Moreover, dual A₁/A_{2A}AR ligands were identified in the group of 1,3-diethyl-7-methylxanthine derivatives. Compound **14b** displayed K_i values of 52.2 nM for the A₁AR and 167 nM for the A_{2A}AR. Selected A_{2A}AR ligands were further evaluated as inactive for inhibition of monoamine oxidase A, B and isoforms of phosphodiesterase-4B1, -10A, which represent classical targets for xanthine derivatives. Therefore, the developed 8-benzylaminoxanthine scaffold seems to be highly selective for AR activity and relevant for potent and selective A_{2A} ligands. Compound **12d** with high selectivity for ARs, especially for the A_{2A}AR subtype, evaluated in animal models of inflammation has shown anti-inflammatory activity. Investigated compounds were found to display high selectivity and may therefore be of high interest for further development as drugs for treating cancer or neurodegenerative diseases.

1. Introduction

Adenosine is an endogenous extracellular signalling molecule involved in the modulation of various physiological and pathological processes. An important source of adenosine is its production by the dephosphorylation of adenosine triphosphate (ATP), which is one of the most abundant molecules in cells [1]. The extracellular functions of adenosine are exerted through adenosine receptor (AR) activation. The ARs belong to the G protein-coupled receptor (GPCR) family and are subdivided into four subtypes: A₁, A_{2A}, A_{2B}, A₃, characterized by coupling to various G protein isoforms, different distribution in tissues and activation by different extracellular concentrations of adenosine [2].

The A₁- and A₃ARs are coupled to G_i proteins resulting in inhibition of adenylyl cyclase, while A_{2A}- and A_{2B}ARs stimulate the enzyme through coupling to G_s proteins. Nevertheless, other second messenger pathways can also be involved in intracellular signal transmission. Their widespread distribution, as well as various cellular responses mediated by modulation of ARs, and, in particular, their roles in diseases, make them potential biological targets for therapeutic application of (un)selective ligands for the different subtypes [3,4].

A_{2A}AR ligands have been investigated in inflammatory, neurological and cardiovascular disorders, among others. High expression of the A_{2A}AR was detected in leukocytes, thymus, spleen, blood platelets and olfactory bulb [5,6]. It is also enriched in heart, lungs, blood vessels

* Corresponding author at: Department of Technology and Biotechnology of Drugs, Jagiellonian University Medical College, 9 Medyczna Street, 30-688 Kraków, Poland.

E-mail address: mfkonono@cyf-kr.edu.pl (K. Kieć-Kononowicz).

<https://doi.org/10.1016/j.bioorg.2020.104033>

Received 24 March 2020; Received in revised form 1 June 2020; Accepted 15 June 2020

Available online 19 June 2020

0045-2068/ © 2020 Published by Elsevier Inc.

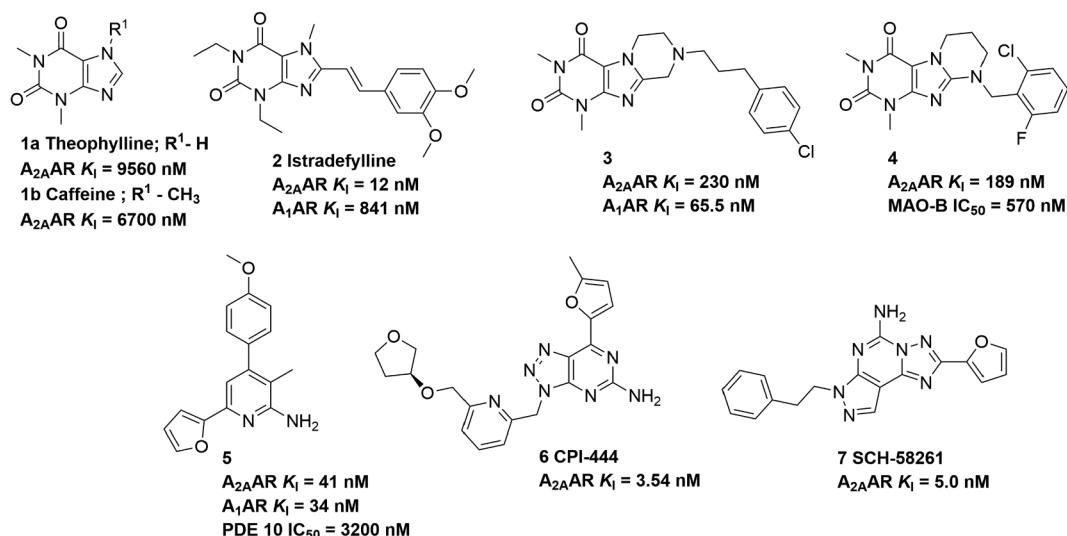


Fig. 1. Adenosine A_{2A}AR antagonists with xanthine and non-xanthine scaffolds [12,15,44,45].

as well as some regions of the brain, especially in striatal nerves [6]. The activation of A_{2A}ARs mediates biological responses through G_s/G_{oif} proteins coupled with adenylate cyclase, and it may also modulate extracellular signal-regulated kinase (ERK) 1/2, c-Jun-N-terminal kinase 1/2 (JNK1/2) [7,8].

Predominantly, the response of peripheral tissues mediated by A_{2A}ARs is associated with protective effects in inflammation and ischemic processes. In those conditions, extracellular adenosine concentrations can rise from basic nanomolar to micromolar levels as a response towards hypoxia or cells damage [4]. As those result, A_{2A}ARs on different immune cells are activated modulating their activity, as well as releasing of various pro- and anti-inflammatory molecules [6,9]. The overall, modulation mediated by A_{2A}ARs results in a down-regulation of immune responses [10,11]. Therefore, A_{2A}AR agonists show strong anti-inflammatory and immunosuppressive effects. Conversely, the blockade of A_{2A}ARs can result in immunostimulatory effects and has therefore been intensively explored with regard to immunotherapy of cancer. Preclinical studies of antitumor activity mediated by a blockade of A_{2A}ARs provided promising outcomes stimulating further development and investigation of A_{2A}AR antagonists [8,12,13].

The intracellular response of A_{2A}AR activation is mediated by an increase in 3',5'-cyclic adenosine monophosphate (cAMP) via adenylate cyclase activation. Therefore, modulation of intracellular level of cAMP in immune cells can also have beneficial effects on antitumor activity. Inhibition of adenylate cyclase isoform 7, as well as activation of phosphodiesterase-4 (PDE-4), an enzyme that hydrolyzes intracellular cAMP, are considered as further promising approaches to protect immune effector cells from adenosine-mediated suppression of antitumor functions [14]. The group of PDE isoforms include 11 families of PDEs (PDE1 – PDE11) with various substrate preferences and biological profiles, and, as mentioned above, modulation of selected isoforms may display potential beneficial effects that enhance therapeutic applications of ARs in inflammatory and neurodegenerative processes [15,16].

Neurodegenerative diseases are another potential application for A_{2A}AR antagonists. There is much evidence indicating their utility in Parkinson disease (PD) as well as Alzheimer disease (AD) [17–20]. In fact, the first A_{2A}AR antagonist, istradefylline, has been approved in Japan, and recently also in the USA for add-on therapy of PD [21,22].

The blockade of A_{2A} can mediate neuroprotective effects, [23] and appear to be beneficial for neuroinflammatory diseases [24,25]. One of the hypotheses explaining the cause of PD is that degradation of dopaminergic neurons of the substantia nigra are associated with

inflammatory processes accompanied by oxidative stress, i.e. increased production of free oxygen radicals [26–28]. According to this hypothesis, a key role in the initiation of brain substantia nigra destruction may be played by microglia [29–33]. The inflammation can cause an activation of microglia, involving an increased production of numerous inflammatory agents: cytokines (TNF- α , interleukin-1), free radicals, and adhesion molecules, which lead to dopaminergic neuron apoptosis [30,31]. Microglia activation is also associated with increased synthesis of nitric oxide and prostaglandin PGJ₂, whose formation is related to cyclooxygenase-2 (COX-2) [34]. These changes promote dopamine oxidation to its quinone derivative which interacts with protein amino acid residues (cysteine, tyrosine, and lysine), leading to their irreversible modification, and reduces cellular glutathione pool, which further increases oxidative stress, causing the death of substantia nigra dopaminergic neurons [35]. Furthermore, activation of A_{2A}ARs decreases dopaminergic transmission of D₂ dopamine receptors, which is detrimental in PD [36,37]. Animal models indicated the potential utility of A_{2A} antagonists in decreasing the formation of β -amyloid plaques as well as in recovering cognitive impairment in AD [38–40].

Despite the above-mentioned effects mediated by A_{2A}AR, there are some hypotheses related to peripheral anti-inflammatory effect of A_{2A}AR antagonists [41,42]. Published papers provided ambiguous results within A_{2A}AR antagonists, that may exhibit anti-inflammatory and antinociceptive effects in mice models [42]. However, those biological effects require further evaluation. So, the functions of A_{2A}ARs in inflammatory processes and the protective effects of A_{2A}AR agonists and antagonists, in the brain and/or in the periphery, are still not fully understood and need further investigations [11].

Due to their immense therapeutic potential, novel molecules acting through A_{2A}ARs are intensively explored in biological studies by medicinal chemists as selective antagonists or as multi target-directed ligands, which combine A_{2A}AR blockade with activity on various biological targets including enzymes and GPCRs to potentiate therapeutic benefits [43,44]. (Fig. 1)

The chemical library of adenosine receptor antagonists consists of xanthine derivatives and non-xanthine ligands. The xanthine-derived antagonists comprise the naturally occurring methylxanthines theophylline (1a), caffeine (1b) with weak subtype selectivity. They are used as central stimulants, for the treatment of sleep apnea, for improving lung functions in preterm babies, as antiasthmatics, and for the treatment of pain in combination with analgesics [45,46].

In the present study, our group developed small molecules containing a xanthine scaffold as selective A_{2A}AR antagonists with various short alkyl substituents at N1, N3, and N7 position and substituted with

benzyl-amino or benzyloxy moieties in the 8-position. Based on our previous results in the group of pyrimido[2,1f]purinedione derivatives, we selected the most promising substitution patterns for high A_{2A} AR affinity creating a new chemical library of compounds derived from 8-benzylaminoxanthine. A principal aim of our efforts was the evaluation of various substitution patterns on the aromatic ring of the benzyl residue and also on the xanthine core with regard to affinity and selectivity for the A_{2A} AR subtype. The structure–activity relationship analysis was additionally supported by molecular docking for human A_{2A} AR. Selected products were tested for ancillary inhibitory activity on the monoamine oxidases (MAO) MAO-A and MAO-B as well as some isoforms of phosphodiesterase (PDE) as potential biological targets since those targets share some mutual pharmacophoric features. Moreover, the most active selective A_{2A} AR ligand was firstly evaluated in metabolic stability studies and then examined in *in vivo* biological experiments including anti-inflammatory, anti-nociceptive and analgesic properties.

2. Results

2.1. Chemistry

The synthetic strategy leading to the target structures is depicted in Schemes 1, 2 and 3. For compounds **9a-h**, **10a-g**, **12a-j**, **15a-e** 8-bromotheophylline, -caffeine or -theobromine were used as starting material. 8-Br-1,3-diethylxanthine (**13d**) was obtained from 1,3-diethylurea (**13a**) and cyanoacetic acid (**13b**) by a modified Traube synthesis approach.

Oxidative bromination was applied for xanthine analogues according to previously described procedures [47,48]. Subsequently, the 8-bromoxanthine derivatives (**11**, **13d**) were alkylated in position N1 or N7 by alkyl bromide (or chloride/iodide) in the presence of K_2CO_3 and DMF as a solvent. The last step leading to the target compounds **9a-h**, **10a-g**, **11a-j**, **14a-c** was performed using microwave irradiation. The 8-bromoxanthine derivatives were treated with the appropriate benzylamine derivatives using triethylamine as a base and 1-propanol as a solvent. Previously developed procedures of microwave irradiation were applied in order to yield the final products which resulted in reduced solvent amount and reaction time compared to conventional heating.

The benzyloxy-substituted compounds **15a-e** were synthesized in analogy to the benzylamino-substituted derivatives but using benzyl alcohols and different reaction conditions in the last step. As a base sodium hydride was applied and DMF was used as a solvent with conventional heating.

For compound **17** 6-amino-1-methyluracil (**16a**) was used as starting material, which was converted to 5,6-diamino-1-methyluracil (**16b**) and subsequently conjugated with glycolic acid leading to 8-

hydroxymethylxanthine (**16c**). The selective alkylation in position N7 was performed using mild reaction conditions with diisopropylethylamine (DIPEA) as a base, and the N1-position was alkylated by iodethane in the presence of K_2CO_3 and DMF at room temperature. 3,7-Dimethyl-1-ethyl-8-hydroxymethylxanthine (**16e**) was treated with PBr_3 to replace the hydroxyl group by a bromine, which enabled the direct conjugation with the appropriate benzylamine derivative in the last synthetic step according to a previously described protocol with some modifications [44].

The structure of all new synthesized compounds was confirmed by spectral analysis including 1H NMR, ^{13}C NMR, and MS. The melting points were determined for the new compounds. The purity of all tested compounds was confirmed to be at least 95% using UPLC coupled to UV/MS.

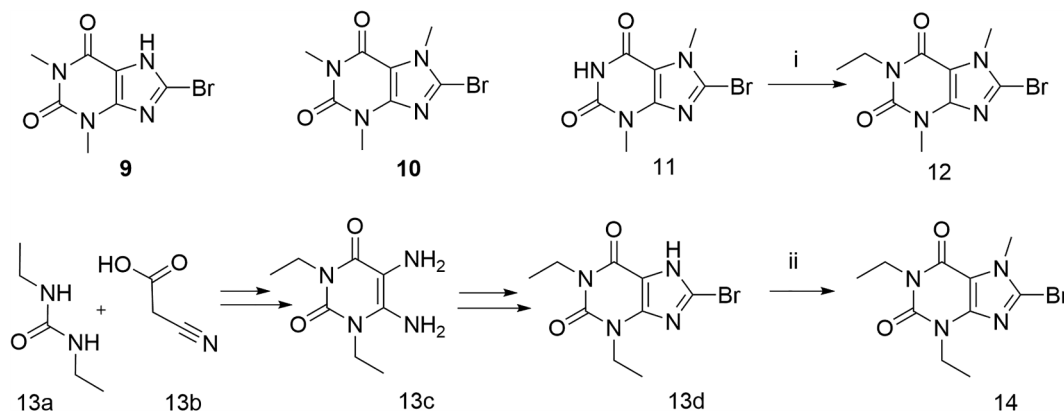
2.2. Biological evaluation

The final compounds were tested in radioligand binding assays to evaluate their affinity for all four ARs subtypes. Human A_1 , A_{2A} , A_{2B} and A_3 ARs were recombinantly expressed in Chinese hamster ovary (CHO) or human embryonic kidney (HEK) cells. [3H]2-Chloro-N⁶-cyclopentyladenosine ([3H]CCPA) [49], [3H]3-(3-hydroxypropyl)-1-propargyl-7-methyl-8-(*m*-methoxystyryl)-xanthine ([3H]MSX-2) [6], [3H]8-(4-(4-(4-chlorophenyl)piperazine-1-sulfonyl)phenyl)-1-propylxanthine ([3H]PSB-603) [50] and [3H]2-phenyl-8-ethyl-4-methyl-(8*R*)-4,5,7,8-tetrahydro-1*H*-imidazo[2,1-*i*]purine-5-one ([3H]PSB-11) [51], respectively, were used as radioligands in A_1 -, A_{2A} -, A_{2B} -, and A_3 AR binding studies. Selected compounds were additionally evaluated for their inhibitory potencies on human MAO-A, MAO-B, PDE-4B1 and PDE-10A. *In vivo* tests for antinociceptive, anti-inflammatory and peripheral analgesic properties were performed.

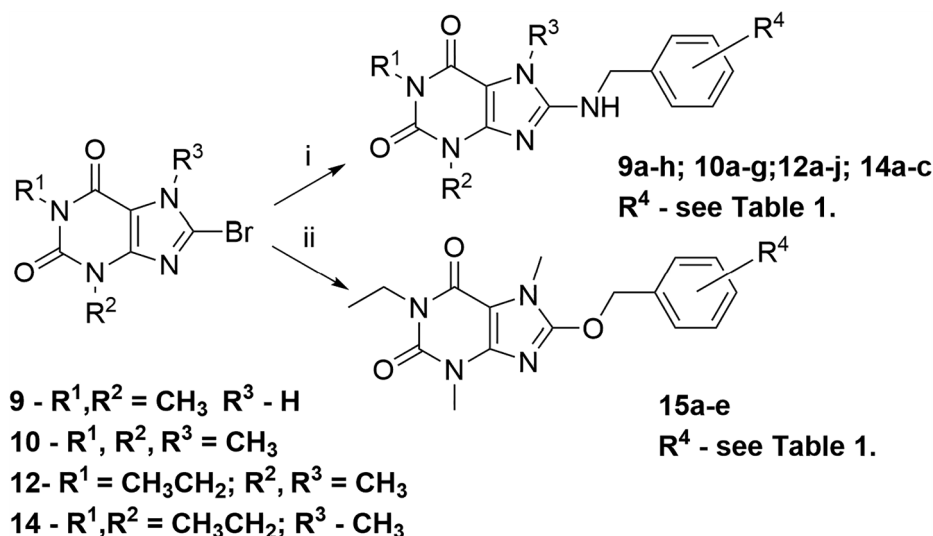
2.3. Structure-activity relationships at adenosine receptors

The presented library of xanthine derivatives combines the same 1,3,7-alkyl substituted xanthine core with a variety of aromatic residues in the 8-position. Therefore, the final compounds can be divided into subgroups with common xanthine cores as depicted in Table 1 presenting their adenosine receptor affinities.

The most potent compounds included **12d** (K_i , A_{2A} AR = 68.5 nM) and **12h** (K_i , A_{2A} AR = 71.1 nM) which belong to the series of 1-ethyl-3,7-dimethylxanthine derivatives. Nevertheless, in each series, potent molecules with affinity in the submicromolar range for the A_{2A} AR were identified. Compounds **14b** (K_i , A_1 AR = 55.0 nM; K_i , A_{2A} AR = 283 nM) and compound **14c** (K_i , A_1 AR = 52.2 nM; K_i , A_{2A} AR = 167 nM) showed dual affinity toward A_1/A_{2A} ARs with higher affinity for the A_1 - than the A_{2A} AR. Moreover, structure **12g** displayed moderate affinity for the A_{2A} AR with ancillary potency at the A_{2B} AR in



Scheme 1. Synthesis of 8-bromoxanthine derivatives; i, ii – K_2CO_3 , DMF, alkyl bromide (or chloride/iodide).



Scheme 2. Synthesis of final structures; i – benzylamine, Et₃N, propanol, μW , ii – benzylalcohol, NaH, DMF.

the submicromolar range (K_i , $A_{2A}AR = 281$ nM; K_i , $A_{2B}AR = 706$ nM). None of the final compounds displayed significant affinity for the A_3AR .

The series of theophylline-based structures showed moderate affinity for the $A_{2A}AR$ of approximately $1 \mu\text{M}$ (K_i value) with lower affinity for the other AR subtypes. An exception was compound **9b** with a *meta*-bromobenzylamino residue in position 8 of the xanthine core displaying additional moderate affinity for the A_1AR (K_i , $A_1AR = 493$ nM; K_i , $A_{2A}AR = 718$ nM). In this series, *meta*-substitution of the aromatic ring appeared to be preferable for high $A_{2A}AR$ affinity. Compounds **9b**, **9f** and **9g** containing chlorine or bromine atoms in the *meta*-position displayed $A_{2A}AR$ affinity in the submicromolar range.

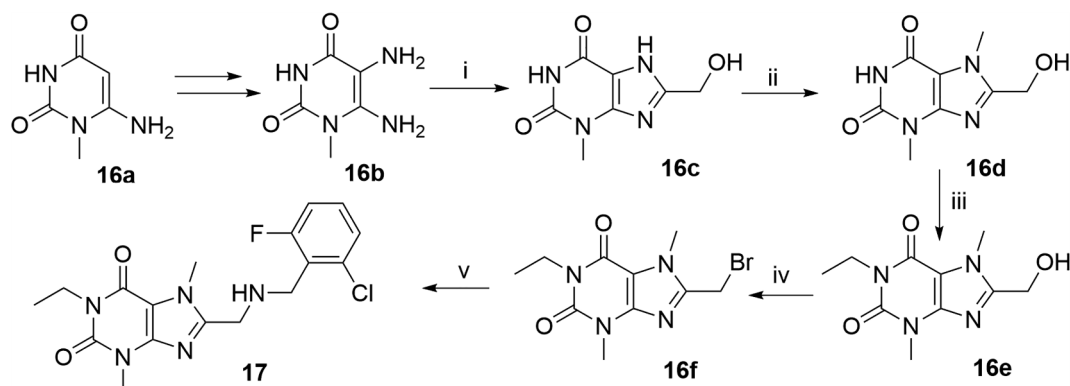
Higher potency and the highest selectivity for the $A_{2A}AR$ were found within the caffeine-derived structures, while for almost all compounds of this series A_1 - A_{2B} -, and A_3AR affinity was very low indicating high $A_{2A}AR$ selectivity. The preferred aromatic substitution was *ortho*-halogen- or -methoxy-benzyl moiety as in **10a**, **10e** and **10f**. Compounds **10a** and **10e** containing a bromine atom or a methoxy group in the *ortho*-position represented the structures with the highest $A_{2A}AR$ affinity of the series with K_i values of 283 nM and 218 nM, respectively.

The $A_{2A}AR$ ligands with the highest affinity were found within the series of 1-ethyl-3,7-dimethylxanthine derivatives. The compounds' selectivity was slightly lower as compared to the caffeine derivatives, nevertheless, it was still high with K_i values at A_1 -, A_{2B} -, and A_3AR s of $> 1 \mu\text{M}$ with one previously mentioned exception, compound **12g** (1-ethyl-8-((2-fluorobenzyl)amino)-3,7-dimethyl-3,7-dihydro-1H-purine-2,6-dione) displaying dual $A_{2A}/A_{2B}AR$ affinity in the nanomolar range.

The best substitution pattern on the aromatic ring for high $A_{2A}AR$ affinity was identical to that observed for the caffeine analogues with the following rank order of potencies: *ortho* > *meta* > *para* for mono-substituted derivatives (halides, methoxy group). The crucial role of *ortho*-substitution was also found in the group of di- and tri-substituted benzyl derivatives. Structures containing an *ortho*-chlorine substituent displayed high affinity for $A_{2A}AR$ even with other halogens or a methoxy group in other positions. Interestingly, compound **12d** containing a 6-chloro-2-fluoro-3-methoxybenzylamino residue in the 8-position showed similar affinity as its *ortho*-chlorobenzylamino-substituted analogue. Additionally, structures **12f** and **12a** with 2,6- or 2,4-di-halogen substitutions of the aromatic ring displayed high affinity for the $A_{2A}AR$ with K_i values of approximately 100 nM and good selectivity versus the other AR subtypes.

Replacement of the amine function in the benzylamino moiety by an oxygen linker in the benzyloxy analogues belonging to the series of 1-ethyl-3,7-dimethylxanthine derivatives resulted in a decrease in affinity for the $A_{2A}AR$ while maintaining selectivity. The most potent compound **15c** (K_i , $A_{2A}AR = 185$ nM) with an *ortho*-bromine substituent on the aromatic ring was slightly (2-fold) more potent than the *ortho*-chlorine analogue **15b** (K_i , $A_{2A}AR = 445$ nM). Nevertheless, comparing structures **15b** and **12h**, the exchange of the amine linker by an oxygen atom decreased the affinity for the $A_{2A}AR$ significantly by about 6-fold.

A change of the AR subtype selectivity profile was observed for the series 1,3-diethyl-7-methylxanthine derivatives. Within the series, a crucial increase in A_1AR affinity while maintaining high affinity the



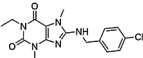
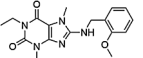
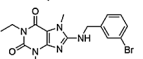
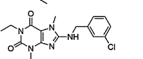
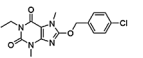
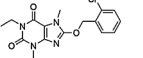
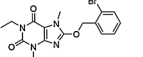
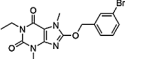
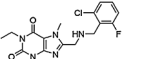
Scheme 3. Synthesis of target compound **17**; i-glycolic acid, NaOH; ii – DIPEA, DMF, iodomethane; iii – iodoethane, K_2CO_3 , DMF; iv – PBr_3 , DCM, v – amine, DIPEA, DCM.

Table 1
Affinities of xanthine derivatives for adenosine receptors.

Compd	R ¹	A ₁ vs. [³ H]CCPA K _i ± SEM (nM) (or % inhibition ± SEM at 1 μM)	A _{2A} vs. [³ H]MSX-2	A _{2B} vs. [³ H]PSB-603	A ₃ vs. [³ H]PSB-11
1b caffeine		44 900	23 400	33 800	13 300
2 istradefylline		841	12	10 000	4700
	N-7-Unsubstituted derivatives				
9a		> 1000 (19 ± 4)	1220 ± 290	> 1000 (13 ± 3)	> 1000 (27 ± 4)
9b		493 ± 157	718 ± 216	> 1000 (37 ± 9)	> 1000 (25 ± 0)
9c		> 1000 (40 ± 2)	> 1000 (46 ± 3)	> 1000 (34 ± 0)	> 1000 (18 ± 2)
9d		> 1000 (23 ± 3)	1380 ± 390	> 1000 (15 ± 3)	> 1000 (15 ± 3)
9e		> 1000 (38 ± 10)	1250 ± 380	> 1000 (4 ± 1)	> 1000 (0 ± 2)
9f		> 1000 (31 ± 9)	768 ± 96	> 1000 (30 ± 0)	> 1000 (24 ± 4)
9g		> 1000 (39 ± 4)	859 ± 55	> 1000 (10 ± 2)	> 1000 (17 ± 2)
9h		> 1000 (24 ± 10)	> 1000 (31 ± 6)	> 1000 (11 ± 3)	> 1000 (8 ± 2)
	N-7-Methylsubstituted derivatives				
10a		> 1000 (13 ± 4)	218 ± 49 (79 ± 2)	> 1000 (-5 ± 3)	> 1000 (-7 ± 2)
10b		> 1000 (23 ± 5)	631 ± 45 (61 ± 3)	> 1000 (-2 ± 2)	> 1000 (-7 ± 2)
10c		> 1000 (6 ± 5)	682 ± 70 (65 ± 3)	> 1000 (0 ± 2)	> 1000 (3 ± 3)
10d		> 1000 (7 ± 3)	789 ± 39 (58 ± 5)	> 1000 (-3 ± 7)	> 1000 (3 ± 1)
10e		> 1000 (7 ± 12)	401 ± 8 (71 ± 5)	> 1000 (0 ± 4)	> 1000 (7 ± 5)
10f		> 1000 (4 ± 7)	283 ± 67 (77 ± 2)	> 1000 (10 ± 2)	> 1000 (-1 ± 1)
10g		> 1000 (25 ± 7)	552 ± 68 (66 ± 2)	> 1000 (12 ± 1)	> 1000 (-1 ± 1)
	N-1-Ethylsubstituted derivatives				
12a		> 1000 (31 ± 10)	148 ± 22 (91 ± 1)	> 1000 (26 ± 1)	> 1000 (5 ± 3)
12b		> 1000 (38 ± 2)	571 ± 271 (68 ± 5)	> 1000 (21 ± 13)	> 1000 (-14 ± 21)
12c		> 1000 (21 ± 14)	419 ± 75 (77 ± 4)	> 1000 (26 ± 1)	> 1000 (9 ± 0)
12d		> 1000 (23 ± 10)	68.5 ± 15.5 (101 ± 2)	> 1000 (46 ± 3)	> 1000 (18 ± 6)
12e		> 1000 (15 ± 11)	1020 ± 224	> 1000 (38 ± 1)	> 1000 (22 ± 1)
12f		> 1000 (36 ± 2)	103 ± 32 (85 ± 4)	> 1000 (31 ± 0)	> 1000 (10 ± 4)
12g		> 1000 (15 ± 7)	281 ± 35 (76 ± 6)	706 ± 112 (44 ± 5)	> 1000 (35 ± 5)
12h		> 1000 (22 ± 8)	71.1 ± 5.8 (88 ± 5)	> 1000 (44 ± 10)	> 1000 (14 ± 1)
12i		> 1000 (39 ± 6)	323 ± 81 (73 ± 2)	> 1000 (31 ± 10)	> 1000 (8 ± 1)

(continued on next page)

Table 1 (continued)

Compd	R ¹	A ₁ vs. [³ H]CCPA K _i ± SEM (nM) (or % inhibition ± SEM at 1 μM)	A _{2A} vs. [³ H]MSX-2	A _{2B} vs. [³ H]PSB-603	A ₃ vs. [³ H]PSB-11
12j		> 1000 (0 ± 1)	> 1000 (39 ± 5)	> 1000 (19 ± 7)	> 1000 (19 ± 1)
	N-1, N-3-Diethylsubstituted derivatives				
14a		240 ± 26 (64 ± 3)	132 ± 9 (99 ± 9)	> 1000 (18 ± 4)	> 1000 (6 ± 1)
14b		52.2 ± 8.5 (86 ± 2)	167 ± 22 (83 ± 4)	> 1000 (33 ± 12)	> 1000 (8 ± 3)
14c		55.0 ± 12.3 (76 ± 2)	283 ± 18 (76 ± 4)	> 1000 (22 ± 8)	> 1000 (16 ± 12)
	8-Benzylloxy derivatives				
15a		> 1000 (9 ± 1)	> 1000 (8 ± 3)	> 1000 (22 ± 4)	> 1000 (-1 ± 4)
15b		> 1000 (34 ± 4)	445 ± 200	> 1000 (24 ± 18)	> 1000 (10 ± 3)
15c		> 1000 (31 ± 5)	185 ± 14	> 1000 (23 ± 1)	> 1000 (9 ± 7)
15d		> 1000 (37 ± 5)	1045 ± 563	> 1000 (9 ± 20)	> 1000 (14 ± 1)
	8-Benzylaminomethyl derivative				
17		> 1000 (15 ± 2)	> 1000 (28 ± 3)	> 1000 (9 ± 6)	> 1000 (-3 ± 1)

A_{2A}AR was discovered. Moreover, *meta*-substitution of the aromatic ring by halogen had a slightly decreasing effect on the affinity for the A_{2A}AR while remarkably improving A₁AR affinity. Compounds **14b** and **14c** (K_i, A₁AR = 52.2 nM; K_i, A_{2A}AR = 167 nM) and (**14c**, A₁AR = 55 nM; K_i, A_{2A}AR = 283 nM) were the most potent dual A₁/A_{2A} AR ligands of the presented chemical library.

Structure **17** can be envisaged as an analogue of **12a** with translocated 2-fluoro-6-chlorobenzylamino residue more distant from the xanthine core by an additional methylene linker in the 8-position. This modification resulted in a significant drop of affinity for A_{2A}AR. This effect may suggest an important role of having a small methyl substituent in the N7-position, as well as some preferences in distance between the aromatic ring in position 8 of the xanthine core with regard to the compounds' affinity for AR subtypes.

2.4. Inhibition of monoamine oxidase A and B

Selected final structures were tested for their inhibitory potency of monoamine oxidase A and B. According to previously published literature, benzylamino-substituted derivatives of tricyclic xanthine derivatives displayed inhibitory activity on MAO-B in the nanomolar range, but were inactive on MAO-A [52]. Therefore, inhibition screening on both, MAO-A and MAO-B, was performed to compare the new library of 8-benzyl-(amino)/(oxy)-xanthine derivatives with the tricyclic xanthines. The results showed very weak activity towards MAO-A and MAO-B for the new xanthine derivatives with inhibition percentage of significantly < 50% at the highest tested concentration (1 μM). The results are collected in Table S1 of [Supplementary Data](#). They clearly indicate selectivity of the tested compounds for ARs versus MAOs.

2.5. Inhibition of phosphodiesterases

According to the previously mentioned role of PDEs on intracellular concentration of cAMP and thus on cAMP-mediated biological

responses, selected compounds were evaluated for their inhibitory potency toward two isoforms of PDE (Table S2 and S3 of [Supplementary Data](#)). PDE-4B1 and PDE-10A were examined in our biological studies due to their potential role in inflammation and/or neurodegenerative disorders being parallel with the application of A_{2A}AR antagonists.

The selected compounds represented the most diverse structural modifications within the synthesized chemical library. All tested structures were only very weak PDE-10A and -4B1 inhibitors. The percent inhibition was not higher than 12% for the most active structure in the highest tested concentration (10 μM).

2.6. Docking to A_{2A}AR crystal structure

Out of a number of available A_{2A}AR crystal structures, paying attention to well described proposed binding interactions of (annulated) xanthines [48], for docking purposes we used the 3REY crystal structure in complex with XAC [53].

For all of the docked ligands, similar putative interaction patterns can be found. The terminal amino group of ASN253^{6.55} is suggested to form a key hydrogen bond with C6 carbonyl group of the purinedione (superscript numbers denote the aminoacids according the Ballesteros-Weinstein numbering system), that itself is located in a narrow pocket formed by PHE168 (ECL2), that stabilizes the system through π-π stacking and GLU169 (ECL2) from one side, and TM7 amino acids MET270^{7.35} and ILE 274^{7.39} from the other side, likely displaying hydrophobic interactions with both of these amino acids. N1-alkyl substituents occupy a small hydrophobic sub-pocket formed by LEU249^{6.51} and MET177^{5.38} on sides, closed at the bottom by HIS250^{6.52}. Halogen substituted aminobenzyl fragment appear to be placed in a subpocket between TM2 apex and EL2, stabilized by hydrogen bond between amine group hydrogen and GLU169. However, in case of methoxy substituted ligands (eg. **12e**) a shift of the benzylamine fragment towards hydrophobic cage of TYR9^{1.35} and TYR271^{7.36} could be observed. This "methoxy shift" in fact might be responsible for twice as high A_{2A}AR affinity of **12d**, when compared to **12a** – by allowing the

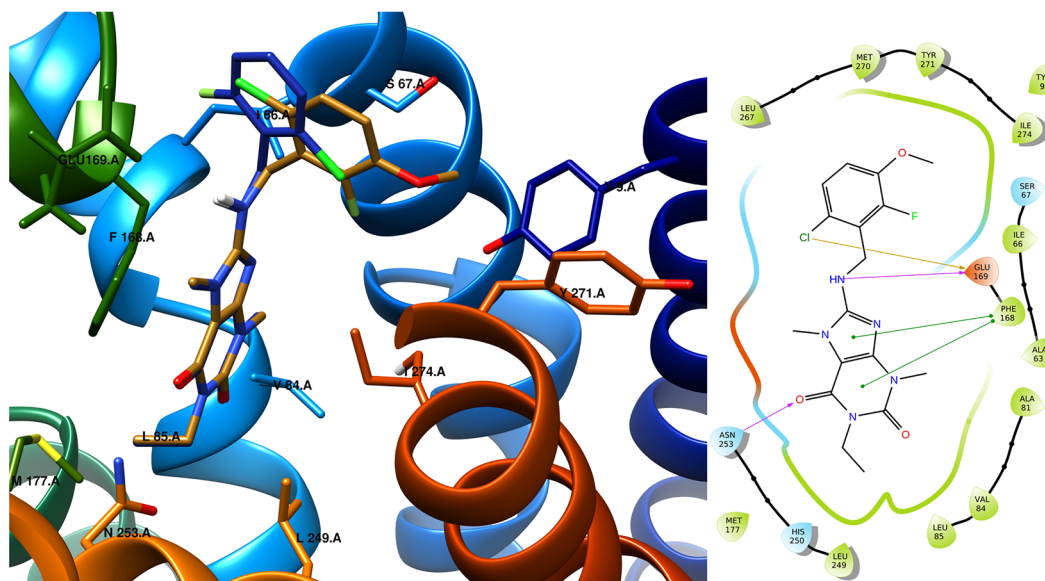


Fig. 2. Putative binding pose of 12a (blue) and 12d (golden) in orthosteric binding pocket of 3REY with corresponding ligand interaction diagram for 12d (left and right panel respectively). ECL3 and partly TM7 residues were removed for better viewing clarity. (For interpretation of the references to color in this figure legend, the reader is referred to the web version of this article.)

halogen bond formation between chlorine atom and GLU169 (Fig. 2). The stability of the calculated poses was evaluated by means of molecular dynamics simulations. Receptor-ligand complexes appeared stable through the whole 600 ps simulation, retaining the key interactions, and the potential energy (U) of the atomic system at the level of ~ 1000 kcal/mol. Furthermore, during the simulation additional arene-H interactions of the substituted benzene ring with SER67^{2,65} and/or ILE274^{7,39} were observed.

2.7. Metabolic stability of compound 12d

To determine the metabolic stability of **12d** in rodents the compound was incubated with mouse (MLMs) and rat liver microsomes (RLMs) for 120 min at 37 °C. The UPLC analyses showed very high metabolic stability of **12d**, as 96.56 and 97.97% of the parent compound remained in the reaction mixtures after incubation with MLMs or RLMs, respectively (Fig. 3). Each performed reaction resulted in the presence of only one metabolite, however depending on the used microsomes the different retention times were observed (5.02 min with MLMs, and 4.80 min with RLMs) (Fig. 3). Indeed, the MS analyses showed different molecular mass of obtained metabolites ($m/z = 382.20$ (MLMs) and $m/z = 368.18$ (RLMs) (Fig. S1 supplementary material)). The prediction of **12d** metabolism performed by MetaSite 6.0.1 showed methoxy- substituent as the most probably site of biotransformation (Fig. 4).

This *in silico* result correlates with the molecular mass of demethylated metabolite obtained by MLMs. The structure of this metabolite was generated *in silico* with very high probability and was presented at Fig. 5A. The molecular mass of the metabolite obtained by RLMs suggests that *N*-deethylation at the xanthine moiety occurred. This metabolite was also predicted *in silico* (Fig. 5B). In conclusion, **12d** was found as very metabolically stable compound in both used species with different main metabolic pathways: demethylation in mice and *N*-deethylation at xanthine moiety in rats.

2.8. Preliminary *in vivo* studies

Compound **12d** was selected for further biological *in vivo* tests being the most potent A_{2A} AR ligand within the presented compound library while showing high AR subtype selectivity as well as selectivity versus

the other evaluated biological targets (MAO-B, PDE-4B1 and -10A). The compound was studied in selected animal models to estimate its anti-inflammatory, antinociceptive and peripheral analgesic properties.

2.8.1. Antinociceptive activity in the formalin test

In the formalin test, which is a model of chronic pain induced by the administration of 5% formalin solution, the evaluated **12d** showed antinociceptive activity (Table 2). **12d** Shortened the licking/biting time of the right hind paw of mice in response to the irritating chemical stimulus.

The injection of formalin into the dorsal surface of the hind paw of a mouse produces a biphasic nocifensive behavioral response, i.e. licking, biting, flinching, or lifting of the injected paw. The acute (neurogenic) nociceptive phase lasts for the first 5 min, and is followed by a period of little activity during the next 10 min. The first phase of the test is directly associated with the stimulation of nociceptors and the development of neurogenic inflammation. The second (late) phase occurs between 15 and 30 min after formalin injection. The second phase is dependent on peripheral inflammation and central sensitization of pain. Since this phase reflects the activation of inflammatory processes, the compounds active in this phase of the experiment have also anti-inflammatory effect.

12d shortened the licking/biting time of the right hind paw of mice only in phase II of the test (15–30 min) (Table 2). The effect was concentration-dependent, and the calculated ED_{50} value for this compound is 31.4 (21.3–42.6) mg/kg b.w. **12d** showed about 4-fold higher activity than reference compound acetyl salicylic acid (ASA) and similar as xanthine derivative **HC-030031** known TRAP1 antagonists [54]. ASA (administered in doses of 50, 100 and 200 mg/kg), attenuated statistically significant pain responses only in the late phases of the formalin test. The calculated ED_{50} value is 126.3 (90.2 – 147.1) mg/kg. While **HC-030031** (administered in doses of 20, 40 and 100 mg/kg), attenuated statistically significant pain responses in the late phases of the formalin test. The calculated ED_{50} value is 33.8 mg/kg. In conclusion, the tested compound demonstrated stronger antinociceptive and anti-inflammatory effect than ASA.

2.8.2. Anti-inflammatory (antiedematous) effect in the carrageenan-induced edema model

12d was administered at a dose of 20 mg/kg body weight.

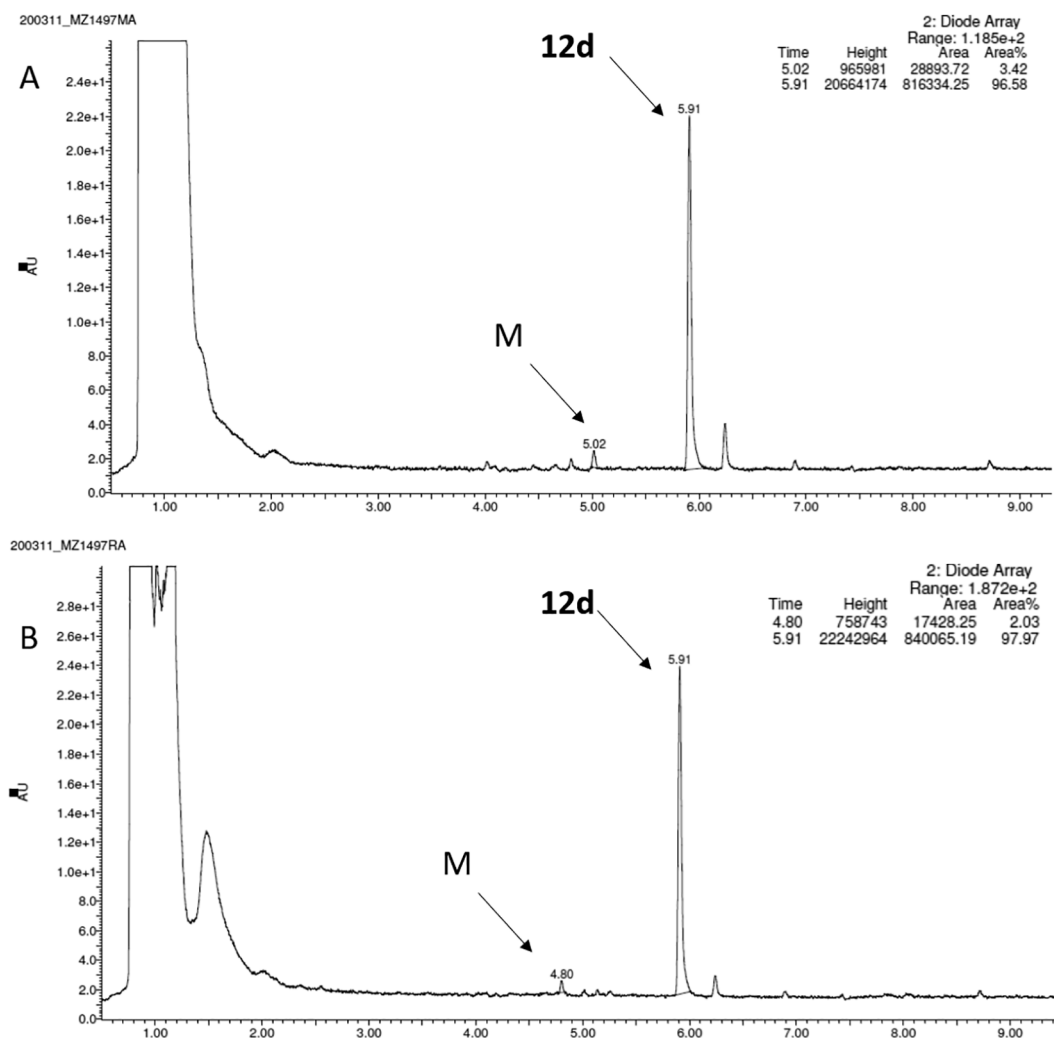


Fig. 3. UPLC spectra after 120 min incubation of compound **12d** with MLMs (A) and RLMs (B).

Ketoprofen was used as a reference compound (Table 3).

The carrageenan test was used to evaluate the anti-inflammatory effect; injection of carrageenan into the hind paw of an animal induces a long-lasting edema. The aim of the present study was to evaluate the anti-inflammatory (antiedematous) activity of **12d**. Ketoprofen administered *ip* at a dose of 20 mg/kg b.w., inhibited edema formation by 23.3%, 54.2% and 66.0% in three consecutive hours of the experiment, respectively.

12d decreased statistically significantly the volume of edema induced by carrageenan injection into the hind paw of rats. A statistically significant effect was observed in the 2nd and 3rd hour of the experiment, inhibiting edema development by 43.8% and 52.8%.

2.8.3. Peripheral analgesic activity of **12d** in the writhing test

The writhing test is a chemical method used to induce pain of peripheral origin by injection of an irritant like phenylbenzoquinone or acetic acid in mice. Analgesic activity of the test compound is inferred from a decrease in the frequency of writhings. This test consists of intraperitoneal injection of the chemical irritant followed by subsequent counting of “writhes”, i.e. characteristic contractions of abdominal muscles accompanied by a hind limb extensor motion. This test detects peripheral analgesic activity; however, some psychoactive agents (including clonidine and haloperidol) also show activity in this test. Compounds with anti-inflammatory properties, such as non-steroidal anti-inflammatory drugs (NSAIDs) show a significant activity in this assay, namely they abolish the reflex stimulated by the administration

of an irritating substance, like phenylbenzoquinone.

Structure **12d** showed analgesic activity (Table 4). Acetylsalicylic acid (ASA) was used as a reference compound.

Statistically significant decrease in the number of writhings was observed by **12d**, showing an analgesic effect; at doses of 5 mg/kg, 10 mg/kg and 20 mg/kg. It reduced the number of writhes in response to phenylbenzoquinone by 32.9%, 54.9% and 82.0%. The ED₅₀ value obtained for **12d** was 8.1 (6.5–10.2) mg/kg b.w. being more potent than that for the reference compound ASA with an ED₅₀ = 39.1 (26.3–49.8) mg/kg b.w. Compound **12d** demonstrated stronger anti-nociceptive effect than ASA.

3. Discussion

In this studies, we investigated a novel library of xanthine derivatives and evaluated their preliminary biological profile, looking for potent and selective A_{2A}AR ligands. The explored scaffold of 8-benzylxanthine was chosen as closely related to N9-benzylpyrimido[2,1-*f*]purinedione derivatives, which were originally designed as bioisosteric analogues of 8-styrylxanthine to overcome some stability drawbacks regarding to styryl fragment.[55,56] The previously reported tricyclic compounds presented dual AR/MAO-B activity with emphasis on MAO-B inhibitory potency.[52] Optimizing the chemical scaffold toward A_{2A}AR activity, the third heterocyclic ring was removed from N9-benzylpyrimido[2,1-*f*]purinedione core providing a novel library of xanthine derivatives. As consequence of structural modification, the

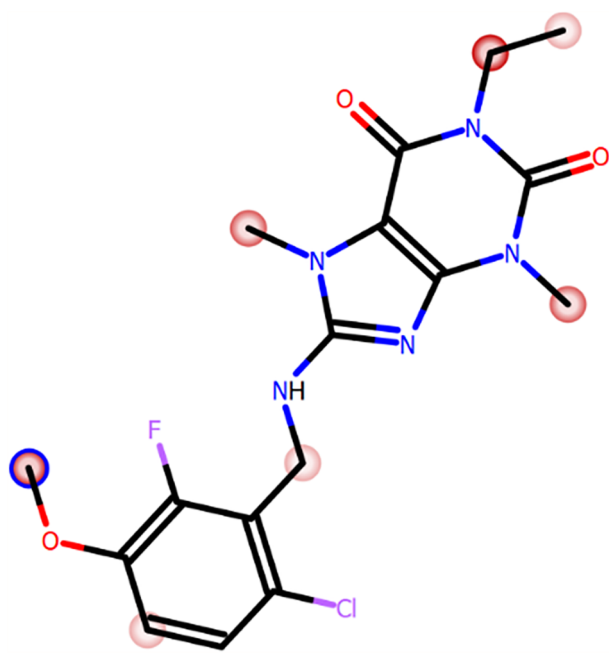


Fig. 4. The MetaSite 6.0.1. software prediction of the most probably sites of compound **12d** metabolism. The darker red color - the higher probability to be involved in the metabolism pathway. The blue circle marked the site of compound with the highest probability of metabolic bioconversion. (For interpretation of the references to color in this figure legend, the reader is referred to the web version of this article.)

designed compounds presented very low inhibitory potencies of MAO-B and higher affinity for A_{2A} AR comparing to the series of N9-benzyl-pyrimido[2,1-*f*]purinedione derivatives. These outcomes indicated important roles of the N7-substituent and the distance between the aromatic residue and the xanthine core on the ability to block MAO-B and MAO-A. Moreover, the 8-benzylaminoxanthine scaffold seems to be more tolerable for AR activity with preference of substitution pattern in

ortho and *meta* position of benzyl moiety. The 10-fold increase of A_{2A} AR affinity was obtained for the most potent ligand **12d** regarding to its tricyclic analogue previously published [52]. The improvement of A_{2A} AR selectivity for **12d** included AR subtypes as well as MAO-B presented classical target for xanthine derivatives.

Although, the A_{2A} AR antagonists are mostly investigated as anti-parkinsonian and antitumor agents as mentioned above, there are some literature evidence that A_{2A} AR antagonists included MSX-3 and unselective caffeine provided anti-inflammatory, antinociceptive and/or analgesic effects in animals models. Moreover, the A_{2A} AR knockout mice show a hypoalgesic phenotype [42,57,58].

Therefore, compound **12d** as the potent and selective A_{2A} ligand was investigated in animal models for anti-inflammatory, antinociceptive and peripheral analgesic properties. Our *in vivo* studies provided outcomes, which were compared to references NSAID such as ASA and ketoprofen. The previous published data characterised those properties within the group of potent and subtype-selective AR antagonists in inflammation and hyperalgesia. The MSX-3, which was used as selective A_{2A} antagonist presented inhibition of formalin or carrageenan induced edema formation, reduction of chemical irritant but not inflammatory pain, and a total block of hyperalgesia in a limited dose range [57].

In the present study, the general effect of **12d** was convergent with effect of MSX-3. Moreover, **12d** showed peripheral analgesic activity in the writhing test. The antinociceptive activity was evaluated as dependent on peripheral inflammation and central sensitization of pain with 4-fold higher activity than reference compound ASA. Moreover, anti-inflammatory effect was additionally detected for **12d** in the carrageenan test. Considering the presented results and literature data, it seems that A_{2A} AR antagonists may display anti-inflammatory, antinociceptive and/or analgesic effects. Moreover, presented biological activities are probably mediated mostly by the selective blockade of A_{2A} AR. The tested structure **12d** was *in vitro* estimated as inactive for another AR subtypes as well as other targets, the modulation of which may produce similar anti-inflammatory response: MAO-B, PDE-4B1 and PDE-10. The further investigation may provide more information and potential utility of those effects related to therapeutically application of A_{2A} AR antagonists.

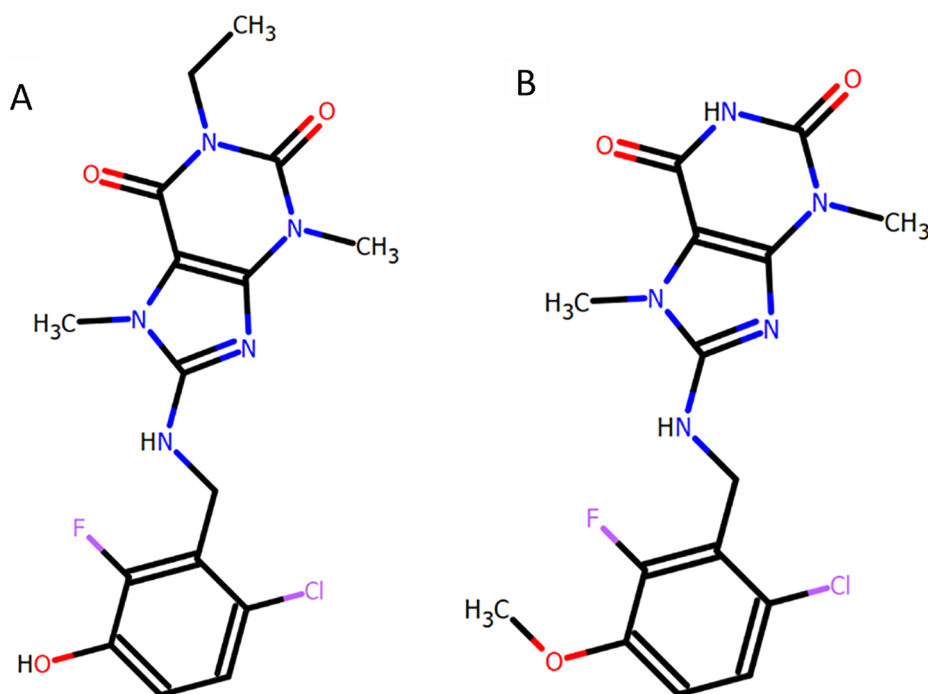


Fig. 5. The *in silico* prediction of the most probable structure of confirmed *in vitro* demethylated **12d** metabolite obtained by MLMs (A) and N-deethylated metabolite obtained by RLMs (B).

Table 2
The influence of **12d** on the duration of pain reaction in the formalin test in mice.

Treatment	Dose [mg/kg]	Licking of the hind paw (sec)		Inhibition [%]	Late phase (15–30 min)	
		Early phase (0–5 min)	Mean \pm SEM		Mean \pm SEM	Inhibition [%]
Control	–		46.2 \pm 1.1	–	181.2 \pm 5.6	–
12d	40		44.8 \pm 0.5	3.1	45.0 \pm 3.4 ^c	75.2
	30		48.8 \pm 0.5	0.0	86.0 \pm 4.1 ^c	52.5
	20		46.5 \pm 0.6	0.0	171.3 \pm 3.3	5.5
Control	–		63.8 \pm 2.03	–	120.8 \pm 3.43	–
ASA	200		62.0 \pm 8.6	9.2	40.6 \pm 14.0 ^b	66.3
	100		58.5 \pm 4.5	14.3	60.3 \pm 9.5 ^b	50.0
	50		59.8 \pm 6.3	12.4	108.7 \pm 13.8	10.0
Control	–		97.0 \pm 6.9	–	158.3 \pm 12.3	–
HC-030031 [54]	100		71.0 \pm 4.1	26.8%	13.9 \pm 1.3 ^c	91.2%
	40		73.8 \pm 5.31	23.8%	76.5 \pm 9.0 ^a	51.7%
	20		82.8 \pm 4.82	14.6%	111.3 \pm 12.2	29.7%

Data are presented as the means \pm SEM of 6–8 mice per group.

^a $p < 0.05$,

^b $p < 0.01$,

^c $p < 0.001$ vs. control.

Table 3
Anti-inflammatory (antiedematous) effect of **12d** in the carrageenan-induced paw edema test.

Treatment	Dose [mg/kg]	Change in edema volume [ml]		
		1 h	2 h	3 h
Control	–	0.42 \pm 0.08	0.89 \pm 0.11	1.25 \pm 0.06
12d	20	0.36 \pm 0.05	0.50 \pm 0.05 ^a	0.59 \pm 0.06 ^b
Ketoprofen	20	0.32 \pm 0.03	0.41 \pm 0.04 ^a	0.43 \pm 0.03 ^b

Data are presented as the means \pm SEM of six to eight animals per group.

^a $p < 0.05$,

^b $p < 0.01$,

Table 4
The effect of the investigated **12d** in the writhing test.

Treatment	Dose [mg/kg]	Number of writhings	Inhibition [%]
		Mean \pm SEM	
Control	–	29.5 \pm 0.3	–
12d	20	5.3 \pm 1.1 ^c	82.0
	10	13.3 \pm 1.0 ^b	54.9
	5	19.8 \pm 1.3 ^a	32.9
Control	–	19.2 \pm 3.2	–
Acetylsalicylic acid	100	3.2 \pm 1.2 ^c	83.3
	50	8.5 \pm 1.3 ^b	55.7
	30	11.2 \pm 2.1	41.6

Data are presented as the means \pm SEM of six to eight mice per group.

^a $p < 0.05$,

^b $p < 0.01$,

^c $p < 0.001$ vs. control.

4. Conclusion

The synthesis and preliminary biological evaluation of a new xanthine-based library of 8-benzyl-substituted derivatives were performed. The compound library represented diversity in substitution patterns of the xanthine core in the N1-, N3-, and N7-positions as well as on the aromatic benzyl residue. The most potent A_{2A}AR structures (**12d** and **12h**) were found in the group of 1-ethyl-3,7-dimethylxanthine derivatives containing *ortho*-halogen substitution on aromatic residue. This structural modification of the explored xanthine derivatives was found to be preferable for high A_{2A}AR potency as well as selectivity. To evaluate interactions with A_{2A}AR of most active structure **12d**, the molecular docking was performed. Comparing the poses of tested library, the substitution pattern of **12d** resulted in a slightly shift of the benzylamine fragment towards the hydrophobic cage, probably being

responsible for high A_{2A}AR affinity. Interestingly, analogues containing a 1,3-diethyl-7-methylxanthine scaffold in which the methyl substituent in position N3 was replaced by an ethyl moiety showed high affinity for the A₁AR while maintaining A_{2A}AR affinity. Compounds **14a-c** displayed a dual A₁/A_{2A}AR affinity profile.

Selected compounds were tested for their inhibitory potency on MAO-A and MAO-B, as well as isoforms 4B1 and 10A of PDE. The potency to inhibit isoforms of PDE and MAO was evaluated for selected compounds showing that the tested molecules all were virtually inactive and therefore showing high selectivity for the ARs.

Finally, compound **12d** as the most potent A_{2A}AR ligand, which was evaluated as metabolic stable, was investigated in *in vivo* models for anti-inflammatory, antinociceptive and peripheral analgesic properties. Surprisingly the molecule was active in all three animal models. The results of the *in vivo* tests as well as the outcomes of *in vitro* assays confirm the hypothesis that *in vivo* activity could be mediated by the A_{2A}AR. Nevertheless, further biological evaluation is required to confirm the biochemical mechanism of the presented *in vivo* properties.

5. Experimental protocols

5.1. Chemistry

5.1.1. Material and methods

All commercially available reagents and solvents were purchased and used without further purification. Melting points (mp.) were determined on a MEL-TEMP II (LD Inc., USA) melting point apparatus and are uncorrected. ¹H NMR spectra were recorded on a Varian Mercury 300 MHz or JEOL FT-NMR 500 MHz apparatus in CDCl₃ or in DMSO-*d*₆. ¹³C NMR data were recorded on 75 MHz on Varian-Mercury-VX 300 MHz PFG or JEOL FT-NMR 500 MHz spectrometer. The *J* values are reported in Hertz (Hz), and the splitting patterns are designated as follows: s (singlet), d (doublet), t (triplet), dd (doublet of doublets), dt (doublet of triplets), quin (quintet), m (multiplet). The purity of the tested compounds was determined (%) on a Waters TQD mass spectrometer coupled with an Waters ACQUITY UPLC system. Retention times (*t*_R) are given in minutes. The reactions were monitored by thin layer chromatography (TLC) using aluminium sheets coated with silica gel 60F254 (Merck) using as developing system dichloromethane/methanol9:1. Spots were detected under UV light.

The synthesis and physicochemical properties of the compounds **9**, **10**, **12**, **14**, and **16c** were reported previously [48,59,60].

5.1.1.1. General procedure for the synthesis of 8-substituted-benzylaminoxanthine derivatives. A mixture of 0.55 mmol of 8-

bromotheophylline (**9**) or 8-bromocaffeine (**10**) or 8-bromo-1-ethyl-3,7-dimethyl-3,7-dihydro-1*H*-purine-2,6-dione (**12**) or 8-bromo-1,3-diethyl-7-methyl-3,7-dihydro-1*H*-purine-2,6-dione (**14**), 1.1 mmol of appropriate benzylamine, 1.6 mmol of TEA and 1.00 mL of propanol was heated in closed vessels in microwave oven (300 Watt, Power Max Off, 150 °C, 10 bar) for 1 h. The solvent was removed and the residue was treated with ethanol. The products were purified by crystallization from ethanol or flash column chromatography over silica gel with CH_2Cl_2 : MeOH (100 : 0 to 80 : 20) as eluent.

5.1.1.1.1. *N*-7-Unsubstituted derivatives. 8-((2-Chlorobenzyl)amino)-1,3-dimethyl-1*H*-purine-2,6(3*H*,7*H*)-dione (**9a**)

Yield: 113 mg; 61%; mp: 243–244 °C; ^1H NMR (300 MHz, DMSO- d_6) δ ppm 3.16 (s, 3H, N1CH₃), 3.33 (s, 3H, N3CH₃), 4.49 (d, J = 6.45 Hz, 2H, NHCH₂), 7.11–7.20 (m, 2H, C5H, C6H, phe), 7.25–7.37 (m, 2H, C3H, C4H, phe), 7.59 (t, J = 6.15 Hz, 1H, NHCH₂), 11.62 (s, 1H, N7H); UPLC/MS purity 96.16%, t_R = 4.80, C₁₄H₁₄ClN₅O₂, MW 319.74, [M + H]⁺ 320.06.

8-((3-Bromobenzyl)amino)-1,3-dimethyl-1*H*-purine-2,6(3*H*,7*H*)-dione (**9b**)

Yield: 110 mg; 53%; mp: 206–207 °C; ^1H NMR (300 MHz, DMSO- d_6) δ ppm 3.16 (s, 3H, N1CH₃), 3.32 (s, 3H, N3CH₃), 4.42 (d, J = 6.45 Hz, 2H, NHCH₂), 7.25–7.35 (m, 2H, C5H, C6H, phe), 7.42 (dt, J = 7.03, 1.76 Hz, 1H, C2H, phe), 7.52 (t, J = 1.76 Hz, 1H, C4H, phe), 7.73 (t, J = 6.45 Hz, 1H, NHCH₂), 11.61 (s, 1H, N7H); UPLC/MS purity 100.00%, t_R = 4.99, C₁₄H₁₄BrN₅O₂, MW 364.20, [M + H]⁺ 364.12.

8-((3,4-Dichlorobenzyl)amino)-1,3-dimethyl-1*H*-purine-2,6(3*H*,7*H*)-dione (**9c**)

Yield: 115 mg; 56%; mp: 202–203 °C; ^1H NMR (300 MHz, DMSO- d_6) δ ppm 3.16 (s, 3H, N1CH₃), 3.32 (s, 3H, N3CH₃), 4.41 (d, J = 7.03 Hz, 2H, NHCH₂), 7.28–7.34 (m, 1H, C2H, phe), 7.55–7.61 (m, 2H, C5H, C6H, phe), 7.73 (t, J = 6.74 Hz, 1H, NHCH₂), 11.64 (s, 1H, N7H); UPLC/MS purity 100.00%, t_R = 5.52, C₁₄H₁₃Cl₂N₅O₂, MW 354.19, [M + H]⁺ 354.02.

8-((2-Bromobenzyl)amino)-1,3-dimethyl-1*H*-purine-2,6(3*H*,7*H*)-dione (**9d**)

Yield: 111 mg; 53%; mp: 206–207 °C; ^1H NMR (500 MHz, DMSO- d_6) δ ppm 3.14 (s, 3H, N1CH₃), 3.30 (s, 3H, N3CH₃), 4.40 (d, J = 6.30 Hz, 2H, NHCH₂), 7.23–7.28 (m, 1H, C5H, phe), 7.29–7.32 (m, 1H, C4H, phe), 7.40 (d, J = 8.02 Hz, 1H, C3H, phe), 7.48–7.52 (m, 1H, C6H, phe), 7.72 (t, J = 6.59 Hz, 1H, NHCH₂), 11.60 (s, 1H, N7H); UPLC/MS purity 100.00%, t_R = 4.91, C₁₄H₁₄BrN₅O₂, MW 364.20, [M + H]⁺ 364.12.

8-((2-Bromo-4-fluorobenzyl)amino)-1,3-dimethyl-1*H*-purine-2,6(3*H*,7*H*)-dione (**9e**)

Yield: 93 mg; 42%; mp: 224–226 °C; ^1H NMR (300 MHz, DMSO- d_6) δ ppm 3.16 (s, 3H, N1CH₃), 3.32 (s, 3H, N3CH₃), 4.44 (d, J = 5.86 Hz, 2H, NHCH₂), 7.25–7.32 (m, 1H, C5H, phe), 7.35–7.41 (m, 1H, C6H, phe), 7.51 (m, 1H, C3H, phe), 7.62 (t, J = 6.15 Hz, 1H, NHCH₂), 11.65 (s, 1H, N7H); UPLC/MS purity 100.00%, t_R = 5.19, C₁₄H₁₃BrFN₅O₂, MW 382.19, [M + H]⁺ 382.00.

8-((3-Bromo-4-fluorobenzyl)amino)-1,3-dimethyl-1*H*-purine-2,6(3*H*,7*H*)-dione (**9f**)

Yield: 121 mg; 55%; mp: 196–197 °C; ^1H NMR (300 MHz, DMSO- d_6) δ ppm 3.16 (s, 3H, N1CH₃), 3.32 (s, 3H, N3CH₃), 4.40 (d, J = 7.03 Hz, 2H, NHCH₂), 7.27–7.41 (m, 2H, C5H, C6H, phe), 7.65 (m, 1H, C2H, phe), 7.71 (t, J = 6.45 Hz, 1H, NHCH₂), 11.60 (br. s., 1H, N7H); UPLC/MS purity 100.00%, t_R = 5.11, C₁₄H₁₃BrFN₅O₂, MW 382.19, [M + H]⁺ 382.07.

8-((3-Chlorobenzyl)amino)-1,3-dimethyl-1*H*-purine-2,6(3*H*,7*H*)-dione (**9g**)

Yield: 99 mg; 51%; mp: 213–214 °C; ^1H NMR (300 MHz, DMSO- d_6) δ ppm 3.16 (s, 3H, N1CH₃), 3.32 (s, 3H, N3CH₃), 4.43 (d, J = 6.45 Hz, 2H, NHCH₂), 7.26–7.39 (m, 4H, C2H, C4H, C5H, C6H, phe), 7.72 (t, J = 6.74 Hz, 1H, NHCH₂), 11.58 (br. s., 1H, N7H); UPLC/MS purity 96.32%, t_R = 4.92, C₁₄H₁₄ClN₅O₂, MW 319.74, [M + H]⁺ 320.25.

8-((4-Chlorobenzyl)amino)-1,3-dimethyl-1*H*-purine-2,6(3*H*,7*H*)-

dione (**9h**)

Yield: 79 mg; 48%; mp: 242–243 °C; ^1H NMR (300 MHz, DMSO- d_6) δ ppm 3.16 (s, 3H, N1CH₃), 3.32 (s, 3H, N3CH₃), 4.41 (d, J = 6.45 Hz, 2H, NHCH₂), 7.31–7.39 (m, 4H, C2H, C3H, C5H, C6H, phe), 7.69 (t, J = 6.45 Hz, 1H, NHCH₂), 11.59 (s, 1H, N7H); UPLC/MS purity 97.70%, t_R = 4.85, C₁₄H₁₄ClN₅O₂, MW 319.74, [M + H]⁺ 320.32.

5.1.1.1.2. *N*-7-Methylsubstituted derivatives. 8-((2-Methoxybenzyl)amino)-1,3,7-trimethyl-3,7-dihydro-1*H*-purine-2,6-dione (**10a**)

Yield: 100 mg; 55%; mp: 251–252 °C; ^1H NMR (400 MHz, CDCl₃) δ ppm 3.37 (s, 3H, N1CH₃) 3.56 (s, 3H, N3CH₃) 3.65 (s, 3H, N7CH₃) 3.91 (s, 3H, OCH₃) 4.66 (d, J = 5.87 Hz, 2H, NHCH₂) 4.90 (br. s., 1H, NHCH₂) 6.91–6.98 (m, 2H, C4H, C5H, phe) 7.29–7.34 (m, 1H, C3H, phe) 7.38 (dd, J = 7.43, 1.96 Hz, 1H, C6H, phe); ^{13}C NMR (CHLOROFORM- d) δ ppm: 27.6 (N1CH₃), 29.5 (N7CH₃), 29.7 (N3CH₃), 43.6 (NHCH₂), 55.4 (OCH₃), 103.2 (C5), 110.5 (C3, phe), 120.7 (C5, phe), 126.1 (C1, phe), 129.3 (C4, phe), 130.1 (C6, phe), 148.5 (C4), 151.8 (C2), 153.4 (C6), 154.2 (C8), 157.6 (C2, phe). UPLC/MS purity 100%; t_R = 5.02; C₁₆H₁₉N₅O₃, MW 329.36; [M]⁺ 330.16.

8-((3-Methoxybenzyl)amino)-1,3,7-trimethyl-3,7-dihydro-1*H*-purine-2,6-dione (**10b**)

Yield: 93 mg; 51%; mp: 197–199 °C; ^1H NMR (300 MHz, DMSO- d_6) δ ppm: 3.13 (s, 3H, N1CH₃) 3.29 (s, 3H, N3CH₃) 3.57 (s, 3H, N7CH₃) 3.71 (s, 3H, OCH₃) 4.49 (d, J = 6.45 Hz, 2H, NHCH₂) 6.76–6.82 (m, 1H, C4H, phe) 6.90–6.95 (m, 2H, C2H, C6H, phe) 7.18–7.26 (m, 1H, C5H, phe) 7.55 (t, J = 6.15 Hz, 1H, NHCH₂); ^{13}C NMR (DMSO- d_6) δ ppm: 27.6 (N1CH₃), 29.7 (N7CH₃), 30.2 (N3CH₃), 46.1 (NHCH₂), 55.4 (OCH₃), 102.4 (C5), 112.7 (C2, phe), 113.5 (C4, phe), 120.0 (C6, phe), 129.8 (C5, phe), 141.6 (C1, phe), 148.6 (C4), 151.6 (C2), 153.3 (C6), 154.4 (C8), 159.7 (C3, phe). UPLC/MS purity 99.4%; t_R = 4.82; C₁₆H₁₉N₅O₃; MW 329.36; [M]⁺ 330.16.

8-((4-Methoxybenzyl)amino)-1,3,7-trimethyl-3,7-dihydro-1*H*-purine-2,6-dione (**10c**)

Yield: 112 mg; 61%; mp: 241–242 °C; ^1H NMR (300 MHz, DMSO- d_6) δ ppm: 3.13 (s, 3H, N1CH₃) 3.30 (s, 3H, N3CH₃) 3.55 (s, 3H, N7CH₃) 3.70 (s, 3H, OCH₃) 4.44 (d, J = 5.86 Hz, 2H, NHCH₂) 6.83–6.89 (m, 2H, C3H, C5H, phe) 7.25–7.31 (m, 2H, C2H, C6H, phe) 7.48 (t, J = 5.86 Hz, 1H, NHCH₂); ^{13}C NMR (DMSO- d_6) δ ppm: 27.6 (N1CH₃), 29.7 (N7CH₃), 30.2 (N3CH₃), 46.1 (NHCH₂), 55.5 (OCH₃), 102.40 (C5), 114.1 (C3/C5, phe), 129.3 (C1/C6, phe), 131.9 (C1, phe), 148.6 (C4), 151.4 (C2), 153.3 (C6), 154.4 (C8), 158.8 (C3, phe). UPLC/MS purity 100%; t_R = 4.77; C₁₆H₁₉N₅O₃; MW 329.36; [M]⁺ 330.16.

8-((3,4-Dimethoxybenzyl)amino)-1,3,7-trimethyl-3,7-dihydro-1*H*-purine-2,6-dione (**10d**)

Yield: 120 mg; 60%; mp: 222–224 °C; ^1H NMR (300 MHz, DMSO- d_6) δ ppm: 3.13 (s, 3H, N1CH₃) 3.31 (s, 3H, N3CH₃) 3.56 (s, 3H, N7CH₃) 3.70 (s, 3H, OCH₃) 3.72 (s, 3H, OCH₃) 4.43 (d, J = 5.86 Hz, 2H, NHCH₂) 6.85–6.88 (m, 2H, C5H, C6H, phe) 7.01 (s, 1H, C2H, phe) 7.48 (t, J = 5.86 Hz, 1H, NHCH₂); ^{13}C NMR (DMSO- d_6) δ ppm: 27.6 (N1CH₃), 29.7 (N7CH₃), 30.2 (N3CH₃), 46.1 (NHCH₂), 55.8 (OCH₃), 56.0 (OCH₃), 102.4 (C5), 112.0 (C2, phe), 112.0 (C5, phe), 120.1 (C6, phe), 132.3 (C1, phe), 148.3 (C4, phe), 148.6 (C4), 148.9 (C3, phe), 151.4 (C2), 153.3 (C6), 154.4 (C8). UPLC/MS purity 98.6%; t_R = 4.30; C₁₇H₂₁N₅O₄; MW 359.39; [M]⁺ 360.14.

8-((2-Chlorobenzyl)amino)-1,3,7-trimethyl-3,7-dihydro-1*H*-purine-2,6-dione (**10e**)

Yield: 83 mg; 45%; mp: 249–251 °C; ^1H NMR (300 MHz, DMSO- d_6) δ ppm: 3.14 (s, 3H, N1CH₃) 3.26 (s, 3H, N3CH₃) 3.62 (s, 3H, N7CH₃) 4.60 (d, J = 5.27 Hz, 2H, NHCH₂) 7.24–7.34 (m, 2H, C4H, C5H, phe) 7.41–7.47 (m, 2H, C3H, C6H, phe) 7.60 (t, J = 5.86 Hz, 1H, NHCH₂); ^{13}C NMR (DMSO- d_6) δ ppm: 27.6 (N1CH₃), 29.7 (N7CH₃), 30.3 (N3CH₃), 43.9 (NHCH₂), 102.6 (C5), 127.6 (C4, phe), 129.2 (C6, phe), 129.6 (C3, phe), 132.5 (C2, phe), 136.9 (C1, phe), 148.5 (C4), 151.3 (C2), 153.4 (C6), 154.2 (C8). UPLC/MS purity 98.1%; t_R = 5.43; C₁₅H₁₆ClN₅O₂; MW 333.78; [M]⁺ 334.15.

8-((2-Bromobenzyl)amino)-1,3,7-trimethyl-3,7-dihydro-1*H*-purine-2,6-dione (**10f**)

Yield: 74 mg; 35%; mp: 251–253 °C; ^1H NMR (300 MHz, DMSO- d_6) δ ppm: 3.14 (s, 3H, N1CH $_3$) 3.27 (s, 3H, N3CH $_3$) 3.63 (s, 3H, N7CH $_3$) 4.56 (d, J = 5.86 Hz, 2H, NHCH $_2$) 7.16–7.25 (m, 1H, C4H, phe) 7.32–7.45 (m, 2H, C5H, C6H, phe) 7.58–7.66 (m, 2H, C3H phe, NHCH $_2$); ^{13}C NMR (DMSO- d_6) δ ppm: 27.6 (N1CH $_3$), 29.8 (N7CH $_3$), 30.4 (N3CH $_3$), 46.4 (NHCH $_2$), 102.7 (C5), 122.8 (C2, phe), 128.2 (C5, phe), 129.4 (C4, phe), 129.5 (C6, phe), 132.8 (C3, phe), 138.4 (C1, phe), 148.6 (C4), 151.4 (C2), 153.4 (C6), 154.2 (C8). UPLC/MS purity 98.6%; t_{R} = 5.58; C $_{15}$ H $_{16}$ BrN $_5$ O $_2$; MW 378.23; [M] $^+$ 378.15.

8-((3-Chlorobenzyl)amino)-1,3,7-trimethyl-3,7-dihydro-1H-purine-2,6-dione (**10g**)

Yield: 88 mg; 48%; mp: 223–224 °C; ^1H NMR (300 MHz, DMSO- d_6) δ ppm: 3.13 (s, 3H, N1CH $_3$) 3.28 (s, 3H, N3CH $_3$) 3.58 (s, 3H, N7CH $_3$) 4.52 (d, J = 5.86 Hz, 2H, NHCH $_2$) 7.26–7.36 (m, 3H, C4H, C5H, C6H, phe) 7.42 (d, J = 1.76 Hz, 1H, C2H, phe) 7.60 (t, J = 6.15 Hz, 1H, NHCH $_2$); ^{13}C NMR (DMSO- d_6) δ ppm: 27.6 (N1CH $_3$), 29.7 (N7CH $_3$), 30.3 (N3CH $_3$), 45.6 (NHCH $_2$), 102.6 (C5), 126.5 (C6, phe), 127.3 (C5, phe), 127.7 (C4, phe), 130.6 (C2, phe), 133.4 (C1, phe), 142.7 (C3, phe), 148.5 (C4), 151.4 (C2), 153.4 (C6), 154.2 (C8). UPLC/MS purity 98.9%; t_{R} = 5.51; C $_{15}$ H $_{16}$ ClN $_5$ O $_2$; MW 333.78; [M] $^+$ 334.15.

5.1.1.1.3. *N*-1-Ethylsubstituted derivatives. 8-((2-Chloro-6-fluorobenzyl)amino)-1-ethyl-3,7-dimethyl-3,7-dihydro-1H-purine-2,6-dione (**12a**)

Yield: 97 mg; 48%; mp: 256–257 °C; ^1H NMR (500 MHz, DMSO- d_6) δ ppm 1.00–1.06 (m, 3H, N1CH $_2$ CH $_3$) 3.32 (br. s., 3H, N3CH $_3$) 3.47–3.52 (m, 3H, N7CH $_3$) 3.78–3.84 (m, 2H, N1CH $_2$) 4.58 (br. s., 2H, NHCH $_2$) 7.21 (t, J = 8.02 Hz, 1H, C4H, phe) 7.27–7.39 (m, 3H, C3H, C5H, phe; NHCH $_2$); UPLC/MS purity 96.8%; t_{R} = 5.87; C $_{16}$ H $_{17}$ ClFN $_5$ O $_2$; MW 365.79; [M] $^+$ 366.18.

8-((3-Chlorobenzyl)amino)-1-ethyl-3,7-dimethyl-3,7-dihydro-1H-purine-2,6-dione (**12b**)

Yield: 104 mg; 54%; mp: 209–211 °C; ^1H NMR (300 MHz, DMSO- d_6) δ ppm 1.05 (t, J = 7.03 Hz, 3H, N1CH $_2$ CH $_3$) 3.29 (s, 3H, N3CH $_3$) 3.59 (s, 3H, N7CH $_3$) 3.83 (q, J = 7.03 Hz, 2H, N1CH $_2$) 4.52 (d, J = 5.86 Hz, 2H, NHCH $_2$) 7.26–7.38 (m, 3H, C4H, C5H, C6H, phe) 7.41 (s, 1H, C2H, phe) 7.61 (t, J = 6.15 Hz, 1H, NHCH $_2$); ^{13}C NMR (DMSO- d_6) δ ppm: 13.8 (N1CH $_2$ CH $_3$), 29.6 (N7CH $_3$), 30.3 (N3CH $_3$), 35.5 (N1CH $_2$), 45.6 (NHCH $_2$), 102.6 (C5), 126.5 (C6, phe), 127.3 (C5, phe), 127.6 (C4, phe), 130.6 (C2, phe), 133.4 (C1, phe), 142.7 (C3, phe), 148.6 (C4), 150.9 (C2), 153.0 (C6), 154.2 (C8). UPLC/MS purity 96.8%; t_{R} = 5.96; C $_{16}$ H $_{18}$ ClN $_5$ O $_2$; MW 347.80; [M] $^+$ 348.17.

8-((3-Bromobenzyl)amino)-1-ethyl-3,7-dimethyl-3,7-dihydro-1H-purine-2,6-dione (**12c**)

Yield: 116 mg; 53%; mp: 216–217 °C; ^1H NMR (300 MHz, CDCl $_3$) δ ppm 1.21 (t, J = 6.74 Hz, 3H, N1CH $_2$ CH $_3$) 3.52 (s, 3H, N3CH $_3$) 3.68 (s, 3H, N7CH $_3$) 4.02 (q, J = 6.64 Hz, 2H, N1CH $_2$) 4.74 (d, J = 5.28 Hz, 2H, NHCH $_2$) 4.94 (br. s., 1H, NHCH $_2$) 7.12–7.21 (m, 1H, C6H, phe) 7.27–7.33 (m, 1H, C5H, phe) 7.47–7.59 (m, 2H, C2H, C4H, phe); ^{13}C NMR (CHLOROFORM- d) δ ppm: 13.4 (N1CH $_2$ CH $_3$), 29.7 (N7CH $_3$), 29.7 (N3CH $_3$), 36.1 (N1CH $_2$), 47.5 (NHCH $_2$), 103.4 (C5), 123.8 (C3, phe), 127.7 (C6, phe), 129.6 (C5, phe), 130.9 (C4, phe), 132.9 (C2, phe), 137.1 (C1, phe), 148.1 (C4), 151.3 (C2), 152.6 (C6), 154.0 (C8). UPLC/MS purity 97.6%; t_{R} = 6.04; C $_{16}$ H $_{18}$ BrN $_5$ O $_2$; MW 392.26; [M] $^+$ 392.10.

8-((6-Chloro-2-fluoro-3-methoxybenzyl)amino)-1-ethyl-3,7-dimethyl-3,7-dihydro-1H-purine-2,6-dione (**12d**)

Yield: 92 mg; 41%; mp: 254–255 °C; ^1H NMR (300 MHz, DMSO- d_6) δ ppm 1.05 (t, J = 6.74 Hz, 3H, N1CH $_2$ CH $_3$) 3.33 (s, 3H, N3CH $_3$) 3.52 (s, 3H, N7CH $_3$) 3.81–3.85 (m, 5H, N1CH $_2$, OCH $_3$) 4.58 (dd, J = 4.69, 1.76 Hz, 2H, NHCH $_2$) 7.09–7.17 (m, 1H, C4H, phe) 7.21–7.27 (m, 1H, C5H, phe) 7.32 (s, 1H, NHCH $_2$); ^{13}C NMR (DMSO- d_6) δ ppm: 13.8 (N1CH $_2$ CH $_3$), 29.6 (N7CH $_3$ /N3CH $_3$), 30.4 (N1CH $_3$), 38.8 (d, $^3J_{\text{C,F}}$ = 4.6 Hz, NHCH $_2$), 56.8 (OCH $_3$), 102.7 (C5), 114.2 (d, $^4J_{\text{C,F}}$ = 2.3 Hz, C5, phe), 124.5 (d, $^2J_{\text{C,F}}$ = 15.0 Hz, C1, phe), 125.1 (d, $^3J_{\text{C,F}}$ = 4.6 Hz, C6, phe), 125.6 (C4, phe), 146.8 (C3, phe), 148.6 (C4), 151.0 (C2), 151.5 (d, $^1J_{\text{C,F}}$ = 252.2 Hz, C6, phe), 153.1 (C6), 153.9 (C8). UPLC/MS purity 95.7%; t_{R} = 5.85; C $_{17}$ H $_{19}$ ClFN $_5$ O $_3$; MW 395.82;

[M] $^+$ 396.16.

8-((3,4-Dimethoxybenzyl)amino)-1-ethyl-3,7-dimethyl-3,7-dihydro-1H-purine-2,6-dione (**12e**)

Yield: 96 mg; 46%; mp: 242–245 °C; ^1H NMR (500 MHz, DMSO- d_6) δ ppm 1.03 (t, J = 6.59 Hz, 3H, N1CH $_2$ CH $_3$) 3.30 (br. s., 3H, N3CH $_3$) 3.54 (s, 3H, N7CH $_3$) 3.68 (br. s., 3H, OCH $_3$) 3.70 (br. s., 3H, OCH $_3$) 3.78–3.83 (m, 2H, N1CH $_2$) 4.39–4.43 (m, 2H, NHCH $_2$) 6.85 (s, 2H, C5H, C6H, phe) 6.99 (br. s., 1H, C2H, phe) 7.45 (br. s., 1H, NHCH $_2$); ^{13}C NMR (DMSO- d_6) δ ppm: 13.9 (N1CH $_2$ CH $_3$), 29.7 (N7CH $_3$), 30.3 (N3CH $_3$), 35.6 (N1CH $_2$), 46.1 (NHCH $_2$), 55.9 (OCH $_3$), 56.1 (OCH $_3$), 102.6 (C5), 112.2 (C2, phe), 112.2 (C5, phe), 120.2 (C6, phe), 132.5 (C1, phe), 148.4 (C4, phe), 148.8 (C4), 149.1 (C3, phe), 151.1 (C2), 153.1 (C6), 154.6 (C8). UPLC/MS purity 100%; t_{R} = 4.75; C $_{18}$ H $_{23}$ N $_5$ O $_4$; MW 373.41; [M] $^+$ 374.23.

8-((2,4-Dichlorobenzyl)amino)-1-ethyl-3,7-dimethyl-1H-purine-2,6(3H,7H)-dione (**12f**)

Yield: 94 mg; 47%; mp: 226–227 °C; ^1H NMR (500 MHz, DMSO- d_6) δ ppm 1.03 (t, J = 7.16 Hz, 3H, N1CH $_2$ CH $_3$), 3.23 (s, 3H, N3CH $_3$), 3.59 (s, 3H, N7CH $_3$), 3.80 (q, J = 6.87 Hz, 2H, N1CH $_2$), 4.53 (d, J = 5.73 Hz, 2H, NHCH $_2$), 7.34–7.37 (m, 1H, C6H, phe), 7.41–7.44 (m, 1H, C5H, phe), 7.56 (d, J = 1.72 Hz, 1H, C3H, phe), 7.60 (t, J = 6.01 Hz, 1H, NHCH $_2$); ^{13}C NMR (DMSO- d_6) δ ppm 13.83 (CH $_3$ CH $_2$), 29.71 (N7CH $_3$), 30.41 (N3CH $_3$), 35.57 (CH $_3$ CH $_2$), 43.59 (NHCH $_2$), 102.83 (C5), 127.81 (C5, phe), 129.08 (C6, phe), 130.87 (C3, phe), 132.81 (C2, phe), 133.54 (C4, phe), 136.28 (C1, phe), 148.60 (C2), 151.01 (C4), 153.17 (C6), 154.08 (C8); UPLC/MS purity 96.99%, t_{R} = 6.75, C $_{16}$ H $_{17}$ Cl $_2$ N $_5$ O $_2$, MW 382.24, [M + H] $^+$ 382.07.

1-Ethyl-8-((2-fluorobenzyl)amino)-3,7-dimethyl-1H-purine-2,6(3H,7H)-dione (**12g**)

Yield: 55 mg; 32%; mp: 194–195 °C; ^1H NMR (500 MHz, DMSO- d_6) δ ppm 1.03 (t, J = 6.87 Hz, 3H, N1CH $_2$ CH $_3$), 3.25 (d, J = 14.89 Hz, 3H, N3CH $_3$), 3.58 (d, J = 12.60 Hz, 3H, N7CH $_3$), 3.77–3.83 (m, 2H, N1CH $_2$), 4.53 (d, J = 5.16 Hz, 2H, NHCH $_2$), 7.07–7.18 (m, 1H, C5H, phe), 7.34–7.46 (m, 2H, C3H, C4H, phe), 7.50–7.64 (m, 2H, C6H, phe, NHCH $_2$); ^{13}C NMR (DMSO- d_6) δ ppm 13.83 (CH $_3$ CH $_2$), 29.71 (N7CH $_3$), 30.41 (N3CH $_3$), 35.57 (CH $_3$ CH $_2$), 43.59 (NHCH $_2$), 102.83 (C5), 115.66 (C3, phe), 127.81 (C5, phe), 129.08 (C4, phe), 130.88 (C6, phe), 132.81 (C1, phe), 136.29 (C2, phe), 148.60 (C2), 151.01 (C4), 153.17 (C6), 154.08 (C8); UPLC/MS purity 100.00%, t_{R} = 5.40, C $_{16}$ H $_{18}$ FN $_5$ O $_2$, MW 331.34, [M + H] $^+$ 332.16.

8-((2-Chlorobenzyl)amino)-1-ethyl-3,7-dimethyl-1H-purine-2,6(3H,7H)-dione (**12h**)

Yield: 101 mg; 56%; mp: 216–217 °C; ^1H NMR (500 MHz, DMSO- d_6) δ ppm 1.03 (t, J = 7.16 Hz, 3H, N1CH $_2$ CH $_3$), 3.24 (s, 3H, N3CH $_3$), 3.60 (s, 3H, N7CH $_3$), 3.77–3.85 (m, 2H, N1CH $_2$), 4.58 (d, J = 5.73 Hz, 2H, NHCH $_2$), 7.22–7.31 (m, 2H, C4H, C5H, phe), 7.38–7.43 (m, 2H, C3H, C6H, phe), 7.57 (t, J = 6.01 Hz, 1H, NHCH $_2$); ^{13}C NMR (DMSO- d_6) δ ppm 13.85 (CH $_3$ CH $_2$), 29.72 (N7CH $_3$), 30.40 (N3CH $_3$), 35.57 (CH $_3$ CH $_2$), 43.97 (NHCH $_2$), 102.78 (C5), 127.69 (C5, phe), 129.22 (C4, phe), 129.42 (C6, phe), 129.65 (C3, phe), 132.60 (C2, phe), 137.01 (C1, phe), 148.67 (C2), 151.03 (C4), 153.15 (C6), 154.27 (C8); UPLC/MS purity 94.96%, t_{R} = 5.92, C $_{16}$ H $_{18}$ ClN $_5$ O $_2$, MW 347.8, [M + H] $^+$ 348.11.

1-Ethyl-8-((2-methoxybenzyl)amino)-3,7-dimethyl-1H-purine-2,6(3H,7H)-dione (**12i**)

Yield: 74 mg; 41%; mp: 218–219 °C; ^1H NMR (500 MHz, DMSO- d_6) δ ppm 1.04 (t, J = 6.87 Hz, 3H, N1CH $_2$ CH $_3$), 3.25 (s, 3H, N3CH $_3$), 3.59 (s, 3H, N7CH $_3$), 3.79 (s, 3H, OCH $_3$), 3.81 (q, J = 7.45 Hz, 2H, N1CH $_2$), 4.48 (d, J = 5.73 Hz, 2H, NHCH $_2$), 6.87 (t, J = 7.45 Hz, 1H, C5H, phe), 6.95 (d, J = 8.02 Hz, 1H, C3H, phe), 7.18–7.24 (m, 2H, C4H, C6H, phe), 7.35 (t, J = 6.01 Hz, 1H, NHCH $_2$); ^{13}C NMR (DMSO- d_6) δ ppm 13.87 (CH $_3$ CH $_2$), 29.75 (N7CH $_3$), 30.38 (N3CH $_3$), 35.56 (CH $_3$ CH $_2$), 41.23 (NHCH $_2$), 55.86 (OCH $_3$), 102.64 (C5), 110.98 (C3, phe), 120.64 (C5, phe), 127.42 (C1, phe), 128.05 (C4, phe), 128.61 (C6, phe), 148.85 (C2), 151.07 (C4), 153.09 (C6), 154.71 (C8), 157.14 (C2, phe); UPLC/MS purity 98.57%, t_{R} = 5.51, C $_{17}$ H $_{21}$ N $_5$ O $_3$, MW 343.38, [M + H] $^+$ 344.19.

8-((4-Chlorobenzyl)amino)-1-ethyl-3,7-dimethyl-1H-purine-2,6(3H,7H)-dione (**12j**)

Yield: 88 mg; 48%; mp: 238–239 °C; ¹H NMR (500 MHz, DMSO-*d*₆) δ ppm 1.03 (t, *J* = 6.87 Hz, 3H, N1CH₂CH₃), 3.26 (s, 3H, N3CH₃), 3.56 (s, 3H, N7CH₃), 3.80 (q, *J* = 6.87 Hz, 2H, CH₂CH₂), 4.48 (d, *J* = 6.30 Hz, 2H, NHCH₂), 7.29–7.38 (m, 4H, C2H, C6H, C3H, C5H, phe), 7.58 (t, *J* = 6.01 Hz, 1H, NHCH₂); ¹³C NMR (DMSO-*d*₆) δ ppm 13.85(CH₂CH₂), 29.71(N7CH₃), 30.33(N3CH₃), 35.56(CH₂CH₂), 45.54(NHCH₂), 102.69(C5), 128.72(C3, C5, phe), 129.77(C2, C6, phe), 131.98(C4, phe), 139.22(C1, phe), 148.70(C2), 151.04(C4), 153.11(C6), 154.38(C2); UPLC/MS purity 100.00%; t_R = 6.01, C₁₆H₁₈ClN₅O₂, MW 347.8, [M + H]⁺ 348.11.

5.1.1.1.4. *N*-1, *N*-3-Diethylsubstituted derivatives. 1,3-Diethyl-8-((2-methoxybenzyl)amino)-7-methyl-3,7-dihydro-1H-purine-2,6-dione (**14a**)

Yield: 87 mg; 44%; mp: 180–181 °C; ¹H NMR (300 MHz, CDCl₃) δ ppm 1.16–1.25 (m, 3H, N1CH₂CH₃) 1.32 (t, *J* = 7.33 Hz, 3H, N3CH₂CH₃) 3.62 (s, 3H, N7CH₃) 3.89 (s, 3H, OCH₃) 4.02 (q, *J* = 7.03 Hz, 2H, N1CH₂) 4.13 (q, *J* = 7.03 Hz, 2H, N3CH₂) 4.63 (d, *J* = 5.86 Hz, 2H, NHCH₂) 4.79–4.86 (m, 1H, NHCH₂) 6.88–6.96 (m, 2H, C4H, C5H, phe) 7.27–7.32 (m, 1H, C3H, phe) 7.37 (dd, *J* = 7.62, 1.76 Hz, 1H, C6H, phe); ¹³C NMR (CHLOROFORM-*d*) δ ppm: 13.4 (N1CH₂CH₃), 13.5 (N3CH₂CH₃), 29.4 (N7CH₃), 36.0 (N1CH₂), 38.3 (N3CH₂), 43.6 (NHCH₂), 55.4 (OCH₃), 103.4 (C5), 110.4 (C3, phe), 120.6 (C5, phe), 126.3 (C1, phe), 129.2 (C4, phe), 130.3 (C6, phe), 148.1 (C4), 150.8 (C2), 153.4 (C6), 154.0 (C8), 157.6 (C2, phe). UPLC/MS purity 100%; t_R = 6.18; C₁₈H₂₃N₅O₃; MW 357.41; [M]⁺ 358.21.

8-((3-Bromobenzyl)amino)-1,3-diethyl-7-methyl-3,7-dihydro-1H-purine-2,6-dione (**14b**)

Yield: 103 mg; 46%; mp: 191–192 °C; ¹H NMR (300 MHz, CDCl₃) δ ppm 1.22 (t, *J* = 7.03 Hz, 3H, N1CH₂CH₃) 1.31 (t, *J* = 7.03 Hz, 3H, N3CH₂CH₃) 3.67 (s, 3H, N7CH₃) 3.98–4.15 (m, 4H, N1CH₂, N3CH₂) 4.62 (d, *J* = 5.27 Hz, 2H, NHCH₂) 4.75–4.82 (m, 1H, NHCH₂) 7.16–7.23 (m, 1H, C6H, phe) 7.28–7.33 (m, 1H, C5H, phe) 7.38–7.44 (m, 1H, C4H, phe) 7.56 (s, 1H, C2H, phe); ¹³C NMR (CHLOROFORM-*d*) δ ppm: 13.5 (N1CH₂CH₃/N3CH₂CH₃), 29.6 (N7CH₃), 36.1 (N1CH₂), 38.4 (N3CH₂), 46.7 (NHCH₂), 103.6 (C5), 122.7 (C3, phe), 126.6 (C6, phe), 130.2 (C5, phe), 130.9 (C4, phe), 131.1 (C2, phe), 140.7 (C1, phe), 147.8 (C4), 150.7 (C2), 152.8 (C6), 154.1 (C8). UPLC/MS purity 100%; t_R = 6.81; C₁₇H₂₀BrN₅O₂; MW 406.28; [M]⁺ 408.12.

8-((3-Chlorobenzyl)amino)-1,3-diethyl-7-methyl-3,7-dihydro-1H-purine-2,6-dione (**14c**)

Yield: 99 mg; 49%; mp: 177–178 °C; ¹H NMR (500 MHz, DMSO-*d*₆) δ ppm 1.03 (t, *J* = 6.87 Hz, 3H, N1CH₂CH₃) 1.11 (t, *J* = 7.16 Hz, 3H, N3CH₂CH₃) 3.56 (s, 3H, N7CH₃) 3.79–3.84 (m, 2H, N1CH₂) 3.88 (q, *J* = 6.87 Hz, 2H, N3CH₂) 4.47 (d, *J* = 5.73 Hz, 2H, NHCH₂) 7.25–7.33 (m, 3H, C4H, C5H, C6H, phe) 7.42 (s, 1H, C2H, phe) 7.61 (t, *J* = 5.73 Hz, 1H, NHCH₂); ¹³C NMR (DMSO-*d*₆) δ ppm: 13.7 (N1CH₂CH₃), 13.9 (N3CH₂CH₃), 30.3 (N7CH₃), 35.5 (N1CH₂), 38.0 (N3CH₂), 45.8 (NHCH₂), 102.9 (C5), 126.8 (C6, phe), 127.4 (C5, phe), 128.0 (C4, phe), 130.6 (C2, phe), 133.4 (C1, phe), 142.8 (C3, phe), 148.1 (C4), 150.5 (C2), 153.2 (C6), 154.4 (C8). UPLC/MS purity 100%; t_R = 6.64; C₁₇H₂₀ClN₅O₂; MW 361.83; [M]⁺ 362.20.

5.1.1.2. *General procedure for the synthesis of 8-(substituted)benzyl-1-ethyl-3,7-dimethyl-3,7-dihydro-1H-purine-2,6-dione derivatives (15a–15d)*. A mixture of 2 mmol 8-bromo-1-ethyl-3,7-dimethyl-3,7-dihydro-1H-purine-2,6-dione (**12**), 2 mmol of appropriate benzyl alcohol, 1.5 mmol of 60% NaH and 14 mL of DMF was heated at 80 °C for 4 h. The mixture was stirred for the next day at room temperature and the product precipitated upon addition of water. For purification, the compounds were crystallized from ethanol or subjected column chromatography over silica gel with CH₂Cl₂ : MeOH (100 : 0 to 80 : 20).

8-((4-Chlorobenzyl)oxy)-1-ethyl-3,7-dimethyl-3,7-dihydro-1H-purine-2,6-dione (**15a**)

Yield: 200 mg; 28%; mp: 148–151 °C; ¹H NMR (400 MHz, DMSO-*d*₆) δ ppm 1.11 (t, *J* = 6.85 Hz, 3H, N1CH₂CH₃) 3.34 (s, 3H, N3CH₃) 3.49 (s, 3H, N7CH₃) 3.88 (q, *J* = 7.04 Hz, 2H, N1CH₂) 5.26 (s, 2H, OCH₂) 7.25 (d, *J* = 8.61 Hz, 2H, C2H, C6H, phe) 7.44 (d, *J* = 8.61 Hz, 2H, C3H, C5H, phe); ¹³C NMR (DMSO-*d*₆) δ ppm: 13.4 (N1CH₂CH₃), 29.5 (N7CH₃), 31.3 (N3CH₃), 36.4 (N1CH₂), 45.4 (OCH₂), 99.2 (C5), 128.3 (C2/C6, phe), 129.4 (C3/C5, phe), 132.6 (C4, phe), 136.3 (C1, phe), 136.6 (C4), 150.3 (C2), 152.1 (C6), 153.1 (C8). UPLC/MS purity 99.35%; t_R = 5.51; C₁₆H₁₇ClN₄O₃; MW 348.79; [M]⁺ 349.

8-((2-Chlorobenzyl)oxy)-1-ethyl-3,7-dimethyl-3,7-dihydro-1H-purine-2,6-dione (**15b**)

Yield: 90 mg; 13%; mp: 126–129 °C; ¹H NMR (400 MHz, DMSO-*d*₆) δ ppm 1.10 (t, *J* = 7.04 Hz, 3H, N1CH₂CH₃) 3.38 (s, 3H, N3CH₃) 3.61 (s, 3H, N7CH₃) 3.88 (q, *J* = 6.91 Hz, 2H, N1CH₂) 5.57 (s, 2H, OCH₂) 7.39–7.47 (m, 2H, C5H, C6H, phe) 7.53–7.56 (m, 1H, C4H, phe) 7.67 (dd, *J* = 7.04, 2.35 Hz, 1H, C3H, phe); ¹³C NMR (DMSO-*d*₆) δ ppm: 13.6 (N1CH₂CH₃), 29.9 (N7CH₃), 30.1 (N3CH₃), 35.8 (N1CH₂), 69.9 (OCH₂), 103.3 (C5), 127.9 (C5, phe), 130.0 (C6, phe), 131.1 (C4, phe), 131.2 (C3, phe), 133.1 (C2, phe), 133.4 (C1, phe), 146.0 (C4), 150.9 (C2), 154.0 (C6), 155.2 (C8). UPLC/MS purity 100%; t_R = 6.90; C₁₆H₁₇ClN₄O₃; MW 348.79; [M]⁺ 349.

8-((2-Bromobenzyl)oxy)-1-ethyl-3,7-dimethyl-3,7-dihydro-1H-purine-2,6-dione (**15c**)

Yield: 145 mg; 18%; mp: 150–152 °C; ¹H NMR (400 MHz, DMSO-*d*₆) δ ppm 1.10 (t, *J* = 6.85 Hz, 3H, N1CH₂CH₃) 3.34 (s, 3H, N3CH₃) 3.62 (s, 3H, N7CH₃) 3.88 (q, *J* = 7.04 Hz, 2H, N1CH₂) 5.54 (s, 2H, OCH₂) 7.33–7.39 (m, 1H, C4H, phe) 7.46 (t, *J* = 7.04 Hz, 1H, C6H, phe) 7.64–7.73 (m, 2H, C3H, C5H, phe); ¹³C NMR (DMSO-*d*₆) δ ppm: 13.6 (N1CH₂CH₃), 29.9 (N7CH₃), 30.1 (N3CH₃), 35.8 (N1CH₂), 72.0 (OCH₂), 103.3 (C5), 123.5 (C2, phe), 128.5 (C5, phe), 131.3 (C3, phe), 133.2 (C4, phe), 134.7 (C6, phe), 146.0 (C4), 150.9 (C2), 150.9 (C1, phe), 154.0 (C6), 155.2 (C8). UPLC/MS purity 100%; t_R = 7.05; C₁₆H₁₇BrN₄O₃; MW 393.24; [M]⁺ 395.

8-((3-Bromobenzyl)oxy)-1-ethyl-3,7-dimethyl-3,7-dihydro-1H-purine-2,6-dione (**15d**)

Yield: 70 mg; 9%; mp: 147–150 °C; ¹H NMR (400 MHz, DMSO-*d*₆) δ ppm 1.11 (t, *J* = 7.04 Hz, 3H, N1CH₂CH₃) 3.39 (s, 3H, N3CH₃) 3.62 (s, 3H, N7CH₃) 3.89 (q, *J* = 7.04 Hz, 2H, N1CH₂) 5.50 (s, 2H, OCH₂) 7.37–7.42 (m, 1H, C5H, phe) 7.57 (m, 2H, C4H, C6H, phe) 7.76 (s, 1H, C2H, phe); ¹³C NMR (DMSO-*d*₆) δ ppm: 13.6 (N1CH₂CH₃), 29.9 (N7CH₃), 30.1 (N3CH₃), 35.8 (N1CH₂), 71.4 (OCH₂), 103.3 (C5), 122.2 (C3, phe), 127.7 (C6, phe), 131.2 (C5, phe), 131.4 (C4, phe), 131.8 (C2, phe), 138.5 (C1, phe), 146.0 (C4), 150.9 (C2), 154.0 (C6), 155.4 (C8). UPLC/MS purity 100%; t_R = 7.09; C₁₆H₁₇BrN₄O₃; MW 393.24; [M]⁺ 395.

5.1.1.3. *Procedure for the synthesis of 8-(((2,6-dichlorobenzyl)amino)methyl)-1-ethyl-3,7-dimethyl-3,7-dihydro-1H-purine-2,6-dione (17)*

5.1.1.3.1. *Synthesis of 1-ethyl-8-(hydroxymethyl)-3,7-dimethyl-3,7-dihydro-1H-purine-2,6-dione (16e)*. A mixture of 10 mmol of 8-(hydroxymethyl)-3-methyl-3,7-dihydro-1H-purine-2,6-dione (**16c**) and 12 mmol of iodomethane, 25 mmol of DIPEA and 10 mL of DMF was heated over night at 40 °C under TLC control. To yield the crude product, water was added to the mixture and the precipitate was filtered off and used to the next reaction. The mixture of ca. 1 g of crude 8-(hydroxymethyl)-3,7-dimethyl-3,7-dihydro-1H-purine-2,6-dione (**16d**), 1.5 equiv. iodoethane, 2.5 equiv. K₂CO₃ and 10 mL DMF was heated at 70 °C for 4 h. To precipitate the product, water was added. The product was purified by flash column chromatography over silica gel with CH₂Cl₂ : MeOH (100 : 0 to 80 : 20).

Yield: 1.02 g; 42%; mp: 249–250 °C; ¹H NMR (300 MHz, DMSO-*d*₆) δ ppm 1.04–1.12 (m, 3H, N1CH₂CH₃) 3.38 (s, 3H, N3CH₃) 3.84–3.92 (m, 5H, N7CH₃, N1CH₂) 4.55 (s, 2H, CH₂OH) 5.59–5.68 (m, 1H, CH₂OH). UPLC/MS purity 93.6%; t_R = 2.64; C₁₀H₁₄N₄O₃; MW 238.25; [M]⁺ 238.92

5.1.1.3.2. *Synthesis of 8-(((2,6-dichlorobenzyl)amino)methyl)-1-ethyl-*

3,7-dimethyl-3,7-dihydro-1H-purine-2,6-dione (17). The synthesis was performed according to previously described procedures [60]. 1-Ethyl-8-(hydroxymethyl)-3,7-dimethyl-3,7-dihydro-1H-purine-2,6-dione (16d) 400 mg was dissolved in dry CH₂Cl₂ and PBr₃ (0.4 mL) was added dropwise at 0 °C. The solution was allowed to warm to rt and stirred for 1 h. Then it was cooled to 0 °C and the excess of PBr₃ was hydrolyzed by addition of saturated aq. NaHCO₃-solution to the pH 7–8. Then, the aqueous layer was extracted with CH₂Cl₂. The organic extracts were combined, dried over Na₂SO₄ and the solvent was removed by rotary evaporation. The residue was dissolved in a mixture of dimethoxyethane (10 mL), DIPEA (0.5 mL) and 2-chloro-6-fluorobenzylamine was added. The solution was stirred overnight at rt. The product was precipitated upon addition of H₂O. For purification, the compound was subjected to flash-chromatography over silica gel with CH₂Cl₂:MeOH (100 : 0 to 80 : 20).

Yield: 300 mg; 47%; mp: 170–171 °C; ¹H NMR (500 MHz, DMSO-*d*₆) δ ppm 1.06 (t, *J* = 6.87 Hz, 3H, N1CH₂CH₃) 2.56 (br. s., 1H, CH₂NHCH₂) 3.34 (s, 3H, N3CH₃) 3.79–3.87 (m, 9H, N7CH₃, N1CH₂, CH₂NHCH₂, CH₂NHCH₂) 7.14 (t, *J* = 8.59 Hz, 1H, C4H, phe) 7.23–7.31 (m, 2H, C3H, C5H, phe); UPLC/MS purity 94.94%; *t*_R = 3.52; C₁₇H₁₉ClFN₅O₂; MW 379.82; [M]⁺ 380.01.

5.2. Biological experiments

5.2.1. Radioligand binding assays at adenosine receptors

Radioligand binding assays were performed as previously described [50]. For assays at all four human AR subtypes, cell membranes of Chinese hamster ovary (CHO) or human embryonic kidney cells (HEK) recombinantly expressing the respective receptors were purchased from PerkinElmer or prepared in our laboratory. The following compounds were employed as radioligands: A₁: [³H]2-chloro-N⁶-cyclopentyladenosine ([³H]CCPA) [49]; A_{2A}: [³H]3-(3-hydroxypropyl)-1-propargyl-7-methyl-8-(*m*-methoxystyryl)xanthine ([³H]MSX-2) [6]; A_{2B}: [³H]8-(4-(4-chlorophenyl)piperazine-1-sulfonyl)phenyl)-1-propylxanthine ([³H]PSB-603) [50]; A₃: [³H]2-phenyl-8-ethyl-4-methyl-(8*R*)-4,5,7,8-tetrahydro-1*H*-imidazo[2,1-*i*]purine-5-one ([³H]PSB-11) [51]. Initially, a single high concentration of compound was tested (typically 1 μM). For potent compounds, full concentration-inhibition curves were determined using different concentrations of test compounds spanning 3 orders of magnitude. At least three independent experiments were performed. Data were analyzed using the PRISM program version 4.0 or higher (Graph Pad, San Diego, CA, USA).

5.2.2. Monoamine oxidase assays

Inhibition activity of compounds was measured by a fluorometric method for detecting monoamine oxidase activity using the Amplex™ Red Monoamine Oxidase Assay (ThermoFisher Scientific A12214) in a 96-well plate. Human recombinant MAO-B and MAO-A enzymes (Sigma Aldrich M7441 and M7316) were used. The assays were conducted as previously described [52,61]

5.2.3. Phosphodiesterase inhibition assays

Tested and reference compounds were dissolved in dimethyl sulfoxide (DMSO) at a concentration of 10 mM and further diluted in assay buffer (10 mM Tris-HCl, 10 mM magnesium chloride and 0.05% Tween-20; pH 7.4). Inhibition of PDE-10A and -4B1 was measured using PDElight HTS cAMP phosphodiesterase assay kit (Lonza) according to manufacturer's recommendations. 10 ng of PDE-10A and 5 ng of PDE-4B1 (BPS Biosciences) in appropriate buffer was incubated with reference and tested compound for 20 min. After incubation the cAMP substrate (final concentration 1.25 μM for PDE-10A and 5 μM for PDE-4B1) was added and incubated for 1 h. Then PDElight AMP Detection Reagent was added and incubated 10 min. All reactions were carried out at 37 °C in white-walled, 96 half area-well plates which were obtained from Perkin Elmer. Luminescence was measured in a multi-function plate reader (POLARstar Omega, BMG Labtech, Germany). The

percentage of inhibition and IC₅₀s were computed using GraphPad Prism Version 6.0 software.

5.2.4. Metabolic stability

In silico experiments of metabolic stability prediction was performed by MetaSite 6.0.1 provided by Molecular Discovery Ltd. The most probable sites of metabolism were predicted by liver computational model and evaluated by *in vitro* studies using mouse or rat liver microsomes. All experiments were performed according to previously described procedures [62,63].

5.3. A_{2A} AR molecular docking studies

Crystal structure of A_{2A}receptor in complex with XAC (PDB ID: 3REY) [53] respectively were imported into MOE v. 2019.01 (ff used - AMBER10:EHT) and prepared using implemented QuikPrep tool: protonation states were generated using Protonate-3D tool, receptor tether strength – 5000, remove water molecules farther than 4.5 Å from ligand [69]. Ligand library was prepared using Conformational Search tool using default settings. 5 lowest energy conformers were then docked to the rigid form of receptor, with site centred on ligand atoms using Wall Constraint (Placement method: Triangle Matcher, 30 poses to retain before refinement, 10 final poses scored GBVI/WSA dG scoring method). Possible binding pocket adaptation in presence of certain ligands was examined using Induced fit refinement protocol. In order to validate the methods used, co-crystallized ligands were redocked to crystal structures. The superposition of the phenylpurinedione cores with the co-crystallized ligands were of high confidence. Dynamics simulations (in time of 600 ps, T = 300 K) were performed using the Nosé-Poincaré-Andersen equations of motion, force field AMBER10:EHT; R-Field 1:80, Cutoff (8,10).

Ligand interaction diagrams were generated using Schrödinger Maestro [70] and MOE, ligand-receptor visualizations were generated using UCSF Chimera [71]

5.4. Pharmacology

5.4.1. Animals

The *in vivo* experiments were carried out on male albino Swiss mice weighing 18–26 g and male rats Wistar weighing 150–180 g. The animals were housed in constant temperature facilities exposed to 12:12 light–dark cycle and maintained on a standard pellet diet and tap water given *ad libitum*. Control and experimental groups consisted of 6–8 animals each. The investigated compounds were administered intraperitoneally (*ip*) in the form of a suspension in 0.5% methylcellulose. Control animals received the equivalent volume of solvent.

All procedures were conducted according to the guidelines of ICLAS (International Council on Laboratory Animals Science) and were approved by The Local Ethics Committee of the Jagiellonian University in Krakow (agreement nr 47/2014).

5.4.2. Statistical analysis

The data are expressed as the mean ± SEM (standard error of the mean). Differences between vehicle control and treatment groups were tested using one- and two-way ANOVA followed by Duncan's multiple comparison test. The difference of means was statistically significant if *p* < 0.05.

5.4.3. The formalin test

The mice were pretreated with the test compound or the vehicle and were allowed to acclimate in Plexiglas observation chambers (20 × 30 × 15 cm) for 30 min before the test. Then, 20 μL of a 5% formalin solution was injected intraplantarly into the right hind paw using a 26-gauge needle. Immediately after formalin injection, the animals were placed individually into glass beakers and were observed during the next 30 min. Time (in seconds) spent on licking or biting of

the injected paw in selected intervals, 0–5, 15–20, 20–25, and 25–30 min, was measured in each experimental group and was an indicator of nociceptive behavior [64]. The ED₅₀ values and their confidence limits were estimated by the method of Litchfield and Wilcoxon [65].

5.4.4. Carrageenan-induced edema model

Rats were divided into four groups, one of them being the control. In order to produce inflammation, 0.1 mL of 1% carrageenan solution in water was injected into the hind paw subplantar tissue of rats, according to the modified method of C. A. Winter [66] and P. Lence [67]. The development of paw edema was measured with a plethysmometer (Plethysmometr 7140, Ugo Basile). Prior to the administration of test substances, paw diameters were measured by dividers and recorded. The investigated compounds were administered at dose of 20 mg/kg, *ip* (as a suspension in methylcellulose), prior to carrageenan injection. Methylcellulose was administered by the same route, to the control group (methylcellulose had no effect on edema, data not shown). After these administrations, paw diameters were measured at 1, 2, and 3 h. The edema % and edema inhibition % were calculated according to the formulas given below.

$$\text{Edema \%} = (N' \times 100)/N$$

$$\text{Edema inhibition \%} = (N - N' \times 100)/N$$

N: paw diameters measured 1, 2 and 3 h after injection of carrageenan to the control group – paw diameters at the beginning. N': paw diameters measured 1, 2, and 3 h after injection of carrageenan to the test groups – paw diameters at the beginning.

5.4.5. The writhing syndrome test

Mice were treated with 0.25 mL of 0.02% phenylbenzoquinone solution 30 min after *ip* administration of the investigated compound or the vehicle. Then the mice were placed individually in glass beakers and 5 min were allowed to elapse. After that period of time each animal was observed for 10 min and the number of characteristic writhes was counted. The analgesic effect of the tested substances was determined by a decrease in the number of writhes observed [68]. The ED₅₀ values and their confidence limits were estimated by the method of Litchfield and Wilcoxon [65].

Declaration of Competing Interest

The authors declared that there is no conflict of interest.

Acknowledgements

Financial support by the National Science Center, Poland [grant based on decision No DEC-2016/23/N/NZ7/00475] and the Jagiellonian University Medical College in Kraków, Poland [grant no. N42/DBS/000039, N42/DBS/000041], are gratefully acknowledged.

Appendix A. Supplementary material

Supplementary data to this article can be found online at <https://doi.org/10.1016/j.bioorg.2020.104033>.

References

- J. Layland, D. Carrick, M. Lee, K. Oldroyd, C. Berry, Adenosine: physiology, pharmacology, and clinical applications, *JACC Cardiovasc. Interv.* 7 (2014) 581–591, <https://doi.org/10.1016/j.jcin.2014.02.009>.
- B.B. Fredholm, I.J. AP, K.A. Jacobson, K.N. Klotz, J. Linden, International Union of Pharmacology. XXV. Nomenclature and classification of adenosine receptors, *Pharmacol. Rev.* 53 (2001) 527–552.
- B.B. Fredholm, Adenosine receptors as drug targets, *Exp. Cell Res.* 316 (2010) 1284–1288, <https://doi.org/10.1016/j.yexcr.2010.02.004>.
- J.-F. Chen, H.K. Eltzschig, B.B. Fredholm, Adenosine receptors as drug targets — what are the challenges? *Nat. Rev. Drug Discov.* 12 (2013) 265–286, <https://doi.org/10.1038/nrd3955>.
- G. Burnstock, A. Verkhatsky, Receptors for Purines and Pyrimidines, in: *Purinergic Signal. Nerv. Syst.*, 2012: pp. 119–244. https://doi.org/10.1007/978-3-642-28863-0_5.
- C.E. Müller, J. Maurinsh, R. Sauer, Binding of [3H]MSX-2 (3-(3-hydroxypropyl)-7-methyl-8-(m-methoxystyryl)-1-propargylxanthine) to rat striatal membranes—a new, selective antagonist radioligand for A(2A) adenosine receptors., *Eur. J. Pharm. Sci.* 10 (2000) 259–65. <https://doi.org/S092809870000646> [pii].
- K.A. Jacobson, Z.G. Gao, Adenosine receptors as therapeutic targets, *Nat. Rev. Drug Discov.* 5 (2006) 247–264, <https://doi.org/10.1038/nrd1983>.
- J. Hatok, P. Racay, Inhibition of A2A adenosine receptor signaling in cancer cells proliferation by the novel antagonist TP455, *Front. Pharmacol.* 7 (2016) 1–13, <https://doi.org/10.1515/bmc-2016-0015>.
- N. Arizmendi, M. Kulka, Adenosine activates G α s proteins and inhibits C3a-induced activation of human mast cells, *Biochem. Pharmacol.* 156 (2018) 157–167, <https://doi.org/10.1016/j.bcp.2018.08.011>.
- J.C. Yu, G. Lin, J.J. Field, J. Linden, Induction of antiinflammatory purinergic signaling in activated human iNKT cells, *JCI Insight.* 3 (2018) 1–12, <https://doi.org/10.1172/jci.insight.91954>.
- C.N. Wilson, S.J. Mustafa, Adenosine Receptors in Health and Disease, Springer, Berlin Heidelberg, Berlin, Heidelberg (2009), <https://doi.org/10.1007/978-3-540-89615-9>.
- S.B. Willingham, P.Y. Ho, A. Hotson, C. Hill, E.C. Piccione, J. Hsieh, L. Liu, J.J. Buggy, I. McCaffery, R.A. Miller, A2AR antagonism with CPI-444 induces Antitumor responses and augments efficacy to anti-PD(L)1 and anti-CTLA-4 in preclinical models, *Cancer Immunol. Res.* 6 (2018) 1136–1149, <https://doi.org/10.1158/2326-6066.CIR-18-0056>.
- T.L. Whiteside, Expert review of anticancer therapy targeting adenosine in cancer immunotherapy : a review of recent progress targeting adenosine in cancer immunotherapy : a review of recent progress, *Expert Rev. Anticancer Ther.* 17 (2017) 527–535, <https://doi.org/10.1080/14737140.2017.1316197>.
- M. Congreve, G.A. Brown, A. Borodovsky, M.L. Lamb, M. Congreve, G.A. Brown, A. Borodovsky, M.L. Lamb, M. Congreve, G.A. Brown, A. Borodovsky, M.L. Lamb, Expert opinion on drug discovery targeting adenosine A 2A receptor antagonism for treatment of cancer, *Expert Opin. Drug Discov.* 00 (2018) 1–7, <https://doi.org/10.1080/17460441.2018.1534825>.
- L. Kalash, C. Val, J. Azuaje, M.I. Loza, F. Svensson, A. Zoufir, L. Mervin, G. Ladds, J. Brea, R. Glen, E. Sotelo, A. Bender, Computer-aided design of multi-target ligands at A1R, A2AR and PDE10A, key proteins in neurodegenerative diseases, *J. Cheminform.* 9 (2017) 67, <https://doi.org/10.1186/s13321-017-0249-4>.
- B.B. Fredholm, Methylxanthines, Springer, Berlin Heidelberg, Berlin, Heidelberg (2011), <https://doi.org/10.1007/978-3-642-13443-2>.
- K. Fuxe, D. Marcellino, D.O. Borroto-Escuela, M. Guescini, V. Fernández-Dueñas, S. Tanganelli, A. Rivera, F. Ciruela, L.F. Agnati, Adenosine-dopamine interactions in the pathophysiology and treatment of CNS disorders, *CNS Neurosci. Ther.* 16 (2010) e18–e42, <https://doi.org/10.1111/j.1755-5949.2009.00126.x>.
- J. Stockwell, E. Jakova, F.S. Cayabyab, Adenosine A1 and A2A receptors in the brain: current research and their role in neurodegeneration, *Molecules* 22 (2017) 1–18, <https://doi.org/10.3390/molecules22040676>.
- B.C. Shook, P.F. Jackson, Adenosine A 2A receptor antagonists and parkinson's disease, *ACS Chem. Neurosci.* 2 (2011) 555–567, <https://doi.org/10.1021/cn2000537>.
- C. Laurent, S. Eddarkaoui, M. Derisbourg, A. Leboucher, D. Demeyer, S. Carrier, M. Schneider, M. Hamdane, C.E. Müller, L. Buee, D. Blum, Beneficial effects of caffeine in a transgenic model of Alzheimer's disease-like tau pathology, *Neurobiol. Aging* 35 (2014) 2079–2090, <https://doi.org/10.1016/j.neurobiolaging.2014.03.027>.
- D.A. Hussar, *New Drugs 2020, part 1, Nursing (Lond.)*. (2019) 1. <https://doi.org/10.1097/01.NURSE.0000651608.77613.29>.
- M. Torti, L. Vacca, F. Stocchi, Istradefylline for the treatment of Parkinson's disease: is it a promising strategy? *Expert Opin. Pharmacother.* 19 (2018) 1821–1828, <https://doi.org/10.1080/14656566.2018.1524876>.
- L. Yu, H.-Y. Shen, J.E. Coelho, I.M. Araújo, Q.-Y. Huang, Y.-J. Day, N. Rebola, P.M. Canas, E.K. Rapp, J. Ferrara, D. Taylor, C.E. Müller, J. Linden, R.A. Cunha, J.-F. Chen, Adenosine A 2A receptor antagonists exert motor and neuroprotective effects by distinct cellular mechanisms, *Ann. Neurol.* 63 (2008) 338–346, <https://doi.org/10.1002/ana.21313>.
- T.C. Frank-Cannon, L.T. Alto, F.E. McAlpine, M.G. Tansey, Does neuroinflammation fan the flame in neurodegenerative diseases? *Mol. Neurodegener.* 4 (2009) 1–13, <https://doi.org/10.1186/1750-1326-4-47>.
- C.J. Barnum, M.G. Tansey, Neuroinflammation and non-motor symptoms: The dark passenger of parkinson's disease? *Curr. Neurol. Neurosci. Rep.* 12 (2012) 350–358, <https://doi.org/10.1007/s11910-012-0283-6>.
- N. Palacios, K.C. Fitzgerald, J.E. Hart, M.G. Weisskopf, M.A. Schwarzschild, A. Ascherio, F. Laden, Particulate matter and risk of parkinson disease in a large prospective study of women, *Environ. Heal.* 13 (2014) 80, <https://doi.org/10.1186/1476-069X-13-80>.
- Y. Tian, Y. Zhang, R. Zhang, S. Qiao, J. Fan, Resolvin D2 recovers neural injury by suppressing inflammatory mediators expression in lipopolysaccharide-induced Parkinson's disease rat model, *Biochem. Biophys. Res. Commun.* 460 (2015) 799–805, <https://doi.org/10.1016/j.bbrc.2015.03.109>.
- E. Valera, M. Mante, S. Anderson, E. Rockenstein, E. Masliah, Lenalidomide reduces microglial activation and behavioral deficits in a transgenic model of Parkinson's disease, *J. Neuroinflammation.* 12 (2015) 93, <https://doi.org/10.1186/s12974-015-0320-x>.

- [29] S. Gyoneva, L. Shapiro, C. Lazo, E. Garnier-Amblard, Y. Smith, G.W. Miller, S.F. Traynelis, Adenosine A2A receptor antagonism reverses inflammation-induced impairment of microglial process extension in a model of Parkinson's disease, *Neurobiol. Dis.* 67 (2014) 191–202, <https://doi.org/10.1016/j.nbd.2014.03.004>.
- [30] S.-P. Fu, J.-F. Wang, W.-J. Xue, H.-M. Liu, B. Liu, Y.-L. Zeng, S.-N. Li, B.-X. Huang, Q.-K. Lv, W. Wang, J.-X. Liu, Anti-inflammatory effects of BHBA in both in vivo and in vitro Parkinson's disease models are mediated by GPR109A-dependent mechanisms, *J. Neuroinflammation.* 12 (2015) 9. <https://doi.org/10.1186/s12974-014-0230-3>.
- [31] M.M. Khan, D. Kempuraj, R. Thangavel, A. Zaheer, Protection of MPTP-induced neuroinflammation and neurodegeneration by Pycnogenol, *Neurochem. Int.* 62 (2013) 379–388, <https://doi.org/10.1016/j.neuint.2013.01.029>.
- [32] E. Lazdon, N. Stoloro, D. Frenkel, Microglia and Parkinson's disease: footprints to pathology, *J. Neural Transm.* (2020), <https://doi.org/10.1007/s00702-020-02154-6>.
- [33] P. Ugalde-Muñiz, I. Fetter-Pruneda, L. Navarro, E. García, A. Chavarría, Chronic systemic inflammation exacerbates neurotoxicity in a parkinson's disease model, *Oxid. Med. Cell. Longev.* 2020 (2020) 1–19, <https://doi.org/10.1155/2020/4807179>.
- [34] M.E. Figueiredo-Pereira, P. Rockwell, T. Schmidt-Glenewinkel, P. Serrano, Neuroinflammation and J2 prostaglandins: linking impairment of the ubiquitin-proteasome pathway and mitochondria to neurodegeneration, *Front. Mol. Neurosci.* 7 (2015), <https://doi.org/10.3389/fnmol.2014.00104>.
- [35] J.J. Gagne, M.C. Power, Anti-inflammatory drugs and risk of Parkinson disease: A meta-analysis, *Neurology.* 74 (2010) 995–1002, <https://doi.org/10.1212/WNL.0b013e3181d5a4a3>.
- [36] M.E. Freitas, S.H. Fox, Nondopaminergic treatments for Parkinson's disease: current and future prospects, *Neurodegener. Dis. Manag.* 6 (2016) 249–268, <https://doi.org/10.2217/nmt-2016-0005>.
- [37] W. Chen, H. Wang, H. Wei, S. Gu, H. Wei, Istradefylline, an adenosine A2A receptor antagonist, for patients with Parkinson's Disease: A meta-analysis, *J. Neurol. Sci.* 324 (2013) 21–28, <https://doi.org/10.1016/j.jns.2012.08.030>.
- [38] A. Kumar, A. Singh, Ekavali, A review on Alzheimer's disease pathophysiology and its management: An update, *Pharmacol. Reports.* 67 (2015) 195–203, <https://doi.org/10.1016/j.pharep.2014.09.004>.
- [39] M. Rivera-Oliver, M. Díaz-Ríos, Using caffeine and other adenosine receptor antagonists and agonists as therapeutic tools against neurodegenerative diseases: a review, *Life Sci.* 101 (2014) 1–9, <https://doi.org/10.1016/j.lfs.2014.01.083>.
- [40] R. Anand, K.D. Gill, A.A. Mahdi, Therapeutics of alzheimer's disease: past, present and future, *Neuropharmacology* 76 (2014) 27–50, <https://doi.org/10.1016/j.neuropharm.2013.07.004>.
- [41] M. Zygumt, K. Golembiowska, A. Drabczyńska, K. Kieć-Kononowicz, J. Sapa, Anti-inflammatory, antioxidant, and antiparkinsonian effects of adenosine A2A receptor antagonists, *Pharmacol. Biochem. Behav.* 132 (2015) 71–78, <https://doi.org/10.1016/j.pbb.2015.02.020>.
- [42] E. Bastia, K. Varani, A. Monopoli, R. Bertorelli, Effects of A1 and A2A adenosine receptor ligands in mouse acute models of pain, *Neurosci. Lett.* 328 (2002) 241–244, [https://doi.org/10.1016/S0304-3940\(02\)00524-4](https://doi.org/10.1016/S0304-3940(02)00524-4).
- [43] F. Núñez, J. Taura, J. Camacho, M. López-Cano, V. Fernández-Dueñas, N. Castro, J. Castro, F. Ciruela, PBF509, an adenosine A2A receptor antagonist with efficacy in rodent models of movement disorders, *Front. Pharmacol.* 9 (2018) 1–10, <https://doi.org/10.3389/fphar.2018.01200>.
- [44] A. Brunschweiler, P. Koch, M. Schlenk, M. Rafahi, H. Radjainia, P. Küppers, S. Hinz, F. Pineda, M. Wiese, J. Hockemeyer, J. Heer, F. Denonne, C.E. Müller, 8-Substituted 1,3-dimethyltetrahydropyrazino[2,1-f]purinediones: Water-soluble adenosine receptor antagonists and monoamine oxidase B inhibitors, *Bioorg. Med. Chem.* 24 (2016) 5462–5480, <https://doi.org/10.1016/j.bmc.2016.09.003>.
- [45] C.E. Müller, K.A. Jacobson, Recent developments in adenosine receptor ligands and their potential as novel drugs, *BBA* 1808 (2011) 1290–1308, <https://doi.org/10.1016/j.bbame.2010.12.017>.
- [46] J. Jiang, C.J. Seel, A. Temirak, V. Namasivayam, A. Arridu, J. Schabikowski, Y. Baqi, S. Hinz, J. Hockemeyer, C.E. Müller, A2B adenosine receptor antagonists with picomolar potency, *J. Med. Chem.* 62 (2019) 4032–4055, <https://doi.org/10.1021/acs.jmedchem.9b00071>.
- [47] A. Drabczyńska, C.E. Müller, J. Karolak-Wojciechowska, B. Schumacher, A. Schiedel, O. Yuzlenko, K. Kieć-Kononowicz, N9-Benzyl-substituted 1,3-dimethyl- and 1,3-dipropyl-pyrimido[2,1-f]purinediones: Synthesis and structure-activity relationships at adenosine A1 and A2A receptors, *Bioorganic Med. Chem.* 15 (2007) 5003–5017, <https://doi.org/10.1016/j.bmc.2007.04.018>.
- [48] E. Szymańska, A. Drabczyńska, T. Karcz, C.E. Müller, M. Köse, J. Karolak-Wojciechowska, A. Fruziński, J. Schabikowski, A. Doroz-Płonka, J. Handzlik, K. Kieć-Kononowicz, Similarities and differences in affinity and binding modes of tricyclic pyrimido- and pyrazinoxanthines at human and rat adenosine receptors, *Bioorg. Med. Chem.* 24 (2016) 4347–4362, <https://doi.org/10.1016/j.bmc.2016.07.028>.
- [49] K.-N. Klotz, M.J. Lohse, U. Schwabe, G. Cristalli, S. Vittori, M. Grifantini, 2-Chloro-N6-[3H]cyclopentyladenosine ([3HCCPA]) - a high affinity agonist radioligand for A1 adenosine receptors, *Naunyn-Schmiedeberg's Arch. Pharmacol.* 340 (1989) 679–683, <https://doi.org/10.1007/BF00717744>.
- [50] T. Borrmann, S. Hinz, D.C.G. Bertarelli, W. Li, N.C. Florin, A.B. Scheiff, C.E. Müller, 1-Alkyl-8-(piperazine-1-sulfonyl)phenylxanthines: Development and Characterization of Adenosine A2B Receptor Antagonists and a New Radioligand with Subnanomolar Affinity and Subtype Specificity, *J. Med. Chem.* 52 (2009) 3994–4006, <https://doi.org/10.1021/jm900413e>.
- [51] C.E. Müller, M. Diekmann, M. Thorand, V. Ozola, [3H]8-Ethyl-4-methyl-2-phenyl-(8R)-4,5,7,8-tetrahydro-1H-imidazo[2,1-i]-purin-5-one ([3H]PSB-11), a novel high-affinity antagonist radioligand for human A3 adenosine receptors, *Bioorganic Med. Chem. Lett.* 12 (2002) 501–503, [https://doi.org/10.1016/S0960-894X\(01\)00785-5](https://doi.org/10.1016/S0960-894X(01)00785-5).
- [52] M. Zatuski, J. Schabikowski, M. Schlenk, A. Olejarz-Maciej, B. Kubas, T. Karcz, K. Kuder, G. Latacz, M. Zygumt, D. Synak, S. Hinz, C.E. Müller, K. Kieć-Kononowicz, Novel multi-target directed ligands based on annelated xanthine scaffold with aromatic substituents acting on adenosine receptor and monoamine oxidase B. Synthesis, in vitro and in silico studies, *Bioorg. Med. Chem.* 27 (2019) 1195–1210, <https://doi.org/10.1016/j.bmc.2019.02.004>.
- [53] A.S. Doré, N. Robertson, J.C. Errey, I. Ng, K. Hollenstein, B. Tehan, E. Hurrell, K. Bennett, M. Congreve, F. Magnani, C.G. Tate, M. Weir, F.H. Marshall, Structure of the adenosine A2A receptor in complex with ZM241385 and the Xanthines XAC and Caffeine, *Structure.* 19 (2011) 1283–1293, <https://doi.org/10.1016/j.str.2011.06.014>.
- [54] G. Chłoń-Rzepa, M. Ślusarczyk, A. Jankowska, A. Gawalska, A. Bucki, M. Kołaczkowski, A. Świerczek, K. Pocięcha, E. Wyska, M. Zygumt, G. Kazek, K. Sałat, M. Pawłowski, Novel amide derivatives of 1,3-dimethyl-2,6-dioxypurin-7-yl-alkylcarboxylic acids as multifunctional TRPA1 antagonists and PDE4/7 inhibitors: a new approach for the treatment of pain, *Eur. J. Med. Chem.* 158 (2018) 517–533, <https://doi.org/10.1016/j.ejmech.2018.09.021>.
- [55] J. Hockemeyer, J.C. Burbiel, C.E. Müller, Multigram-scale syntheses, stability, and photoreactions of A2A adenosine receptor antagonists with 8-styrylxanthine structure: potential drugs for parkinson's disease, *J. Org. Chem.* 69 (2004) 3308–3318, <https://doi.org/10.1021/jo0358574>.
- [56] A. Drabczyńska, T. Karcz, E. Szymańska, M. Köse, C.E. Müller, M. Paskaleva, J. Karolak-Wojciechowska, J. Handzlik, O. Yuzlenko, K. Kieć-Kononowicz, Synthesis, biological activity and molecular modelling studies of tricyclic alkylimidazo-, pyrimido- and diazepinopurinediones, *Purinergic Signal.* 9 (2013) 395–414, <https://doi.org/10.1007/s11302-013-9358-3>.
- [57] A. Bilkei-Gorzo, O.M. Abo-Salem, A.M. Hayallah, K. Michal, C.E. Müller, A. Zimmer, Adenosine receptor subtype-selective antagonists in inflammation and hyperalgesia, *Naunyn-Schmiedeberg's Arch. Pharmacol.* 377 (2008) 65–76, <https://doi.org/10.1007/s00210-007-0252-9>.
- [58] O.M. Abo-Salem, A.M. Hayallah, A. Bilkei-Gorzo, B. Filipek, A. Zimmer, C.E. Müller, Antinociceptive effects of novel A2B adenosine receptor antagonists, *J. Pharmacol. Exp. Ther.* 308 (2004) 358–366, <https://doi.org/10.1124/jpet.103.056036>.
- [59] A. Drabczyńska, O. Yuzlenko, M. Köse, M. Paskaleva, A.C. Schiedel, J. Karolak-Wojciechowska, J. Handzlik, T. Karcz, K. Kuder, C.E. Müller, K. Kieć-Kononowicz, Synthesis and biological activity of tricyclic cycloalkylimidazo-, pyrimido- and diazepinopurinediones, *Eur. J. Med. Chem.* 46 (2011) 3590–3607, <https://doi.org/10.1016/j.ejmech.2011.05.023>.
- [60] P. Koch, A. Brunschweiler, V. Namasivayam, S. Ullrich, A. Maruca, B. Lazzaretto, P. Küppers, S. Hinz, J. Hockemeyer, M. Wiese, J. Heer, S. Alcaro, K. Kieć-Kononowicz, C.E. Müller, Probing substituents in the 1- and 3-position: tetrahydropyrazino-annulated water-soluble xanthine derivatives as multi-target drugs with potent adenosine receptor antagonistic activity, *Front. Chem.* 6 (2018), <https://doi.org/10.3389/fchem.2018.00206>.
- [61] A. Stöfel, M. Schlenk, S. Hinz, P. Küppers, J. Heer, M. Gütschow, C.E. Müller, Dual targeting of adenosine A2A receptors and monoamine oxidase B by 4H–3,1-benzothiazin-4-ones, *J. Med. Chem.* 56 (2013) 4580–4596, <https://doi.org/10.1021/jm400336x>.
- [62] M. Zatuski, K. Stanuch, T. Karcz, S. Hinz, G. Latacz, E. Szymańska, J. Schabikowski, A. Doroz-Płonka, J. Handzlik, A. Drabczyńska, C.E. Müller, K. Kieć-Kononowicz, Tricyclic xanthine derivatives containing a basic substituent: adenosine receptor affinity and drug-related properties, *Medchemcomm.* 9 (2018) 951–962, <https://doi.org/10.1039/c8md00070k>.
- [63] K. Szczepańska, T. Karcz, A. Siwek, K.J. Kuder, G. Latacz, M. Bednarski, M. Szafarz, S. Hagenow, A. Lubelska, A. Olejarz-Maciej, M. Sobolewski, K. Mika, M. Kotańska, H. Stark, K. Kieć-Kononowicz, Structural modifications and in vitro pharmacological evaluation of 4-pyridyl-piperazine derivatives as an active and selective histamine H3 receptor ligands, *Bioorg. Chem.* 91 (2019) 103071, <https://doi.org/10.1016/j.bioorg.2019.103071>.
- [64] Y. Kolesnikov, M. Cristea, G. Oksman, A. Torosjan, R. Wilson, Evaluation of the tail formalin test in mice as a new model to assess local analgesic effects, *Brain Res.* 1029 (2004) 217–223, <https://doi.org/10.1016/j.brainres.2004.09.058>.
- [65] J.T. Litchfield, F. Wilcoxon, A simplified method of evaluating dose-effect experiments, *J. Pharmacol. Exp. Ther.* 96 (1949) 99–113.
- [66] C.A. Winter, E.A. Risley, G.W. Nuss, Carrageenin-Induced Edema in Hind Paw of the Rat as an Assay for Antiinflammatory Drugs, *Exp. Biol. Med.* 111 (1962) 544–547, <https://doi.org/10.3181/00379727-111-27849>.
- [67] P. Lence, A new device for plethysmoscopic measuring of small objects, *Arch. Int. Pharmacodyn. Ther.* 136 (1962) 237–240.
- [68] L.C. Hendershot, J. Forsaith, Antagonism of the frequency of phenylquinone-induced writhing in the mouse by weak analgesics and nonanalgesics, *J. Pharmacol. Exp. Ther.* 125 (1959) 237–240 <http://www.ncbi.nlm.nih.gov/pubmed/13642264>.
- [69] Molecular Operating Environment (MOE), 2019.01; <https://www.chemcomp.com/> (last accessed 09.03.2020).
- [70] Schrödinger Release 2019-1: Schrödinger, LLC, New York, NY, 2019.
- [71] E.F. Pettersen, T.D. Goddard, C.C. Huang, G.S. Couch, D.M. Greenblatt, E.C. Meng, T.E. Ferrin, UCSF Chimera—a visualization system for exploratory research and analysis, *J. Comput. Chem.* 25 (2004) 1605–1612.